



EPTT 2012

SÃO PAULO

Bypass transition and stability theory

Peter Schmid

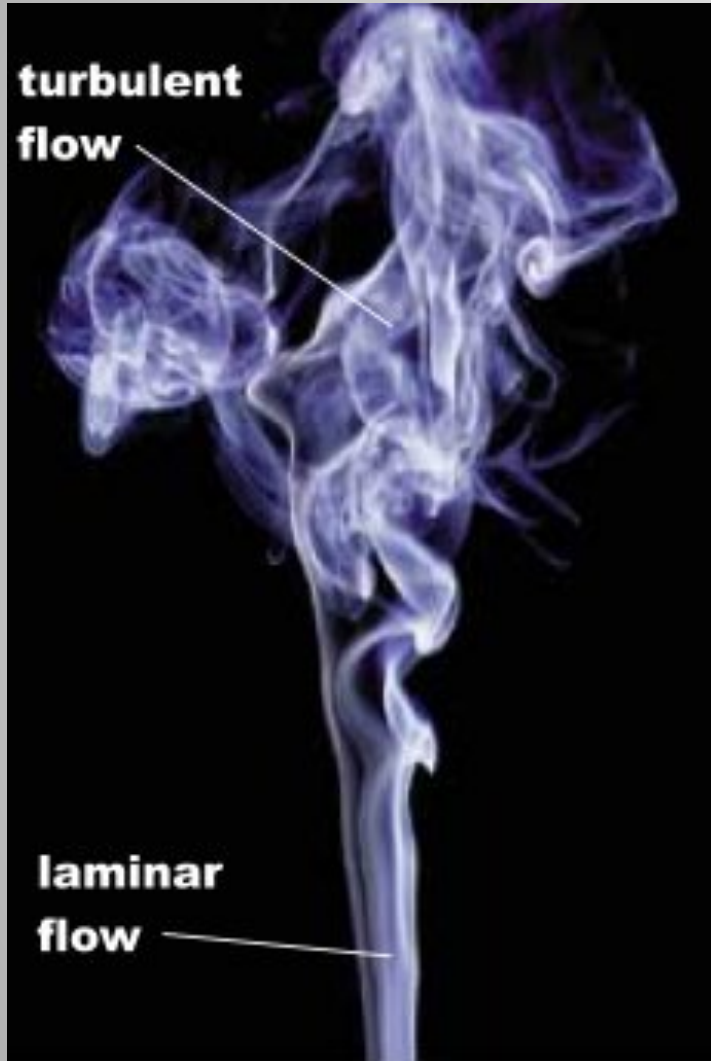
Laboratoire d'Hydrodynamique (LadHyX)

CNRS-Ecole Polytechnique, Palaiseau

EPTT, Sao Paulo, Sept. 2012



Transition to turbulence

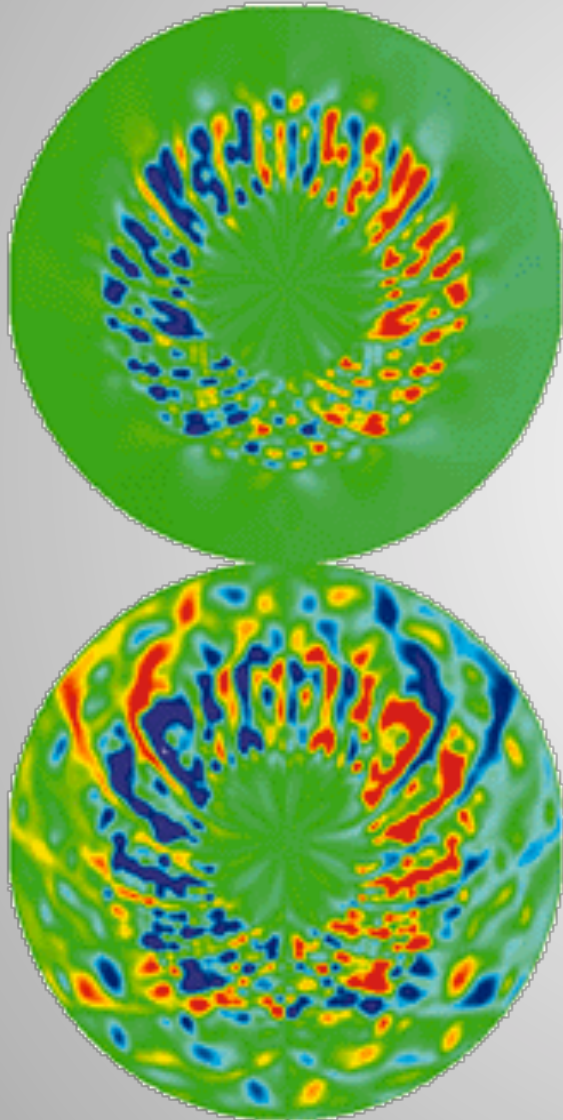


Transition to turbulence

- is a multi-faceted, complex physical process.
- critically depends on the disturbance environment.
- is difficult to classify into « subprocesses ».
- is parameter-dependent.
- is important for the design of fluid systems.

buoyancy-driven flow

Transition to turbulence

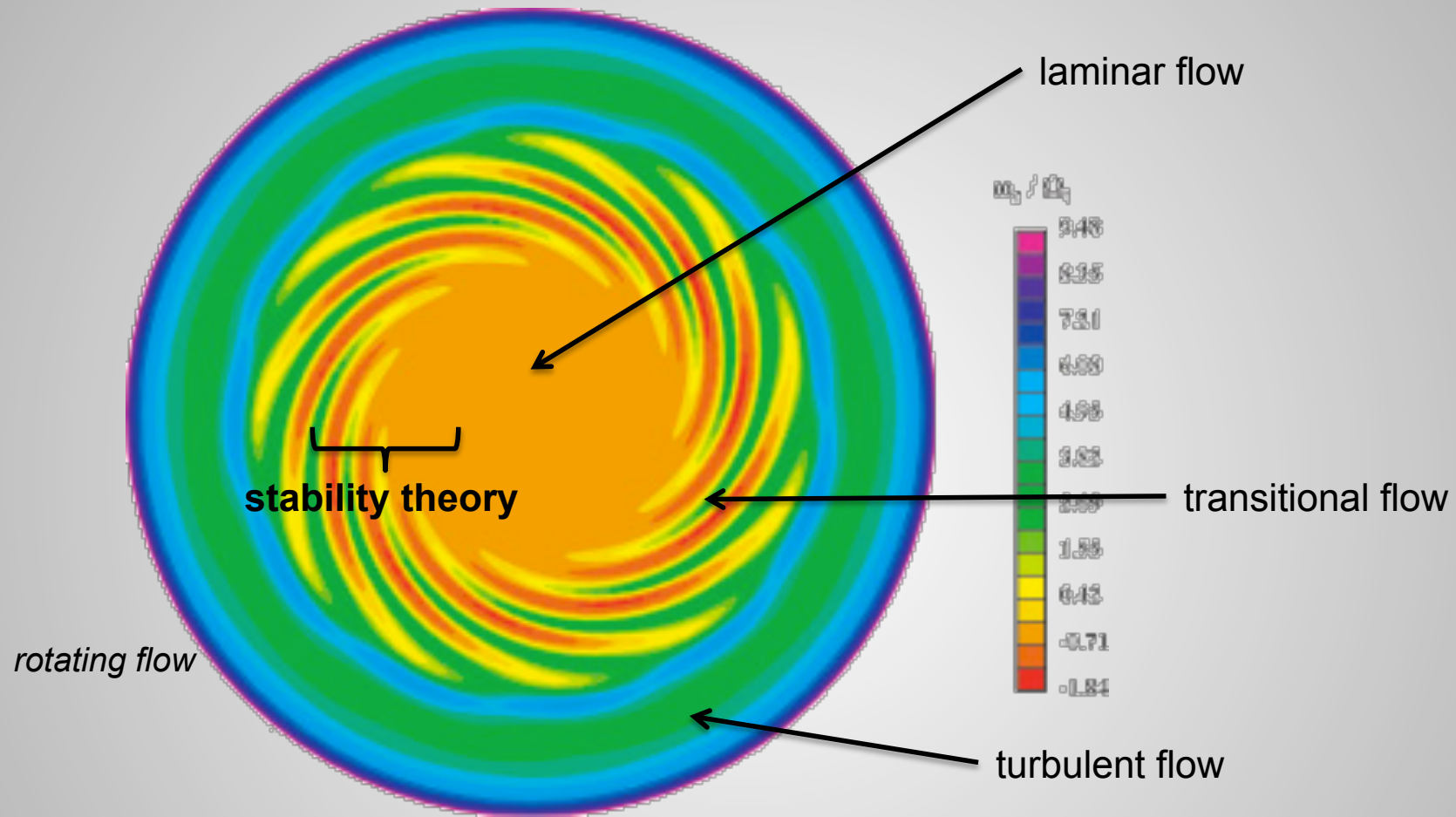


Transition to turbulence

- is a multi-faceted, complex physical process.
- critically depends on the disturbance environment.
- is difficult to classify into « subprocesses ».
- is parameter-dependent.
- is important for the design of fluid systems.

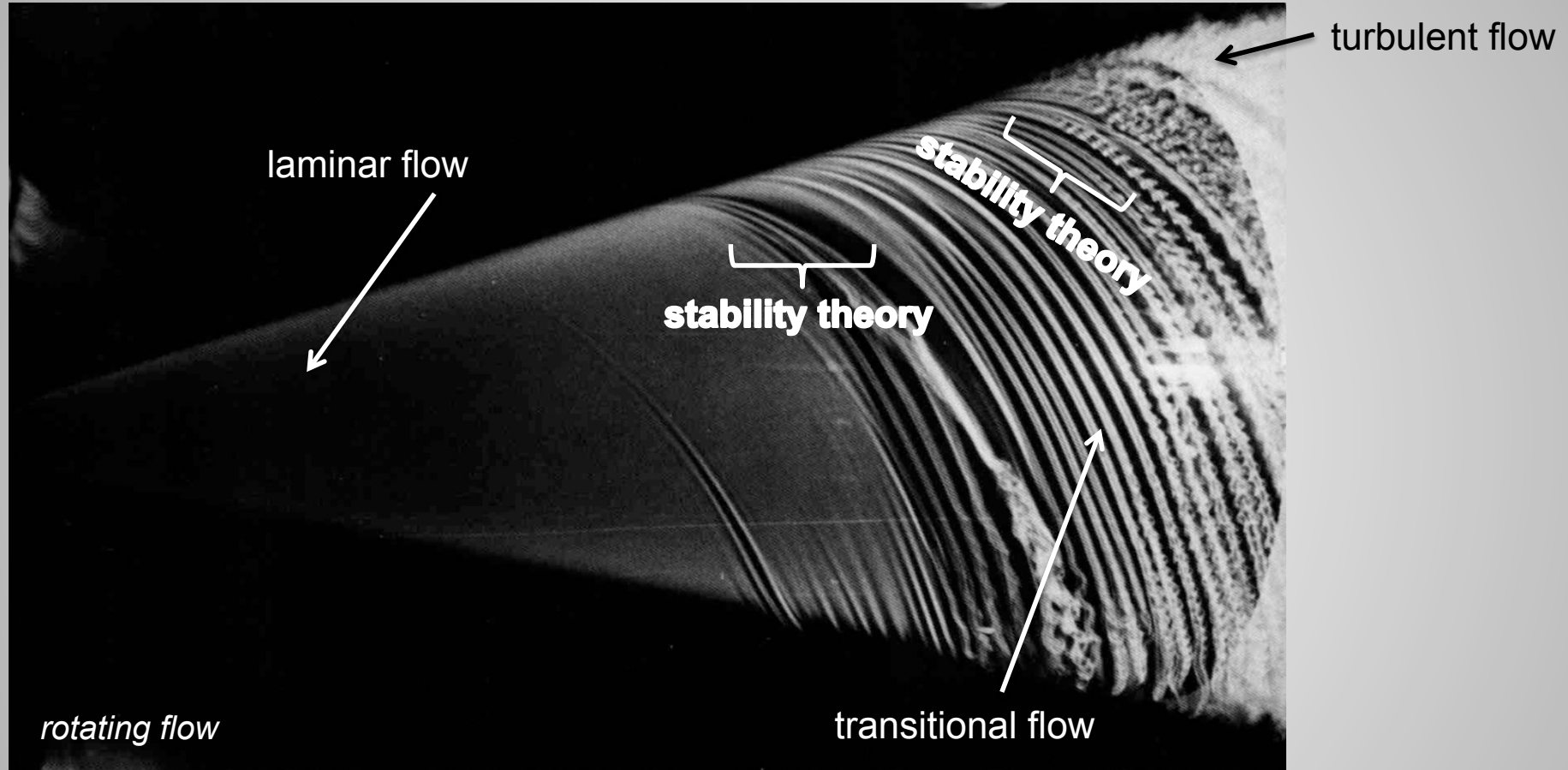
*magnetically driven
Tokamak plasma flow*

Transition to turbulence



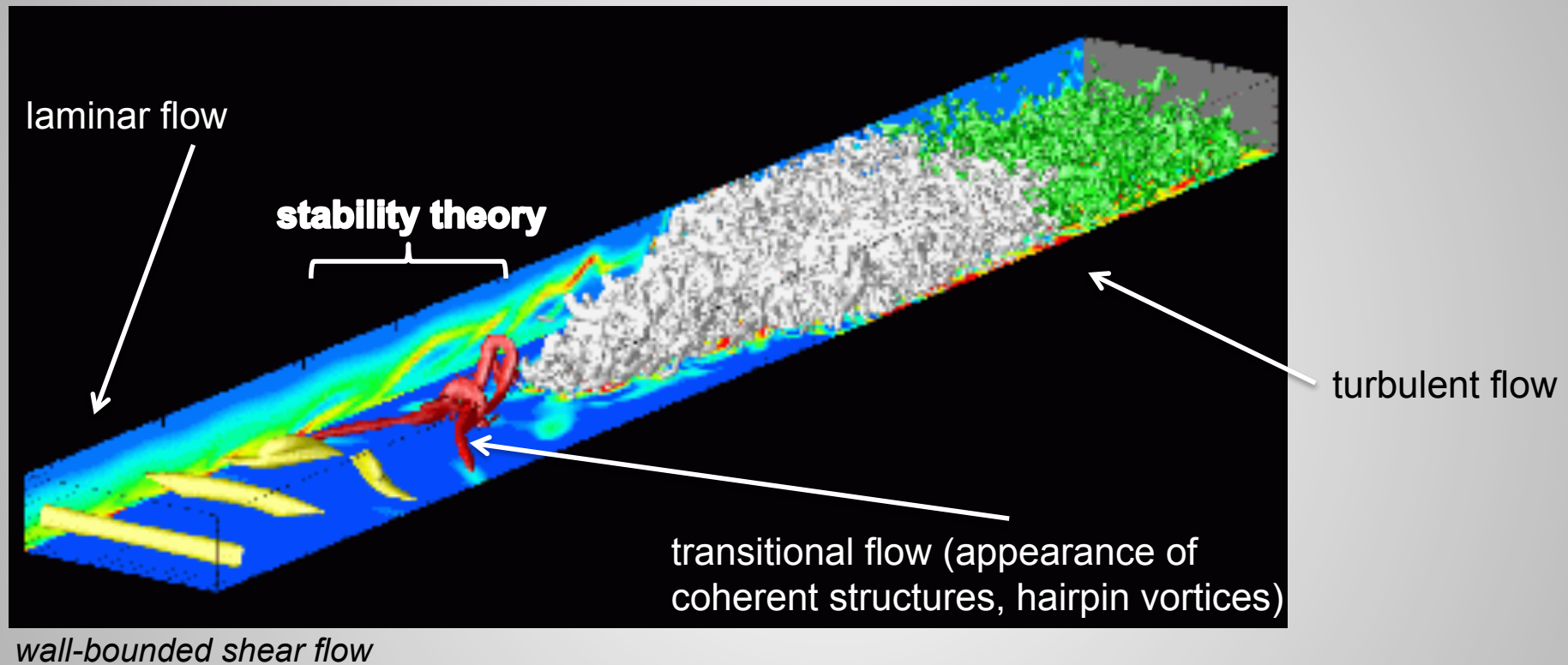
Transition to turbulence has traditionally been described by a sequence of (linear) instabilities.

Transition to turbulence



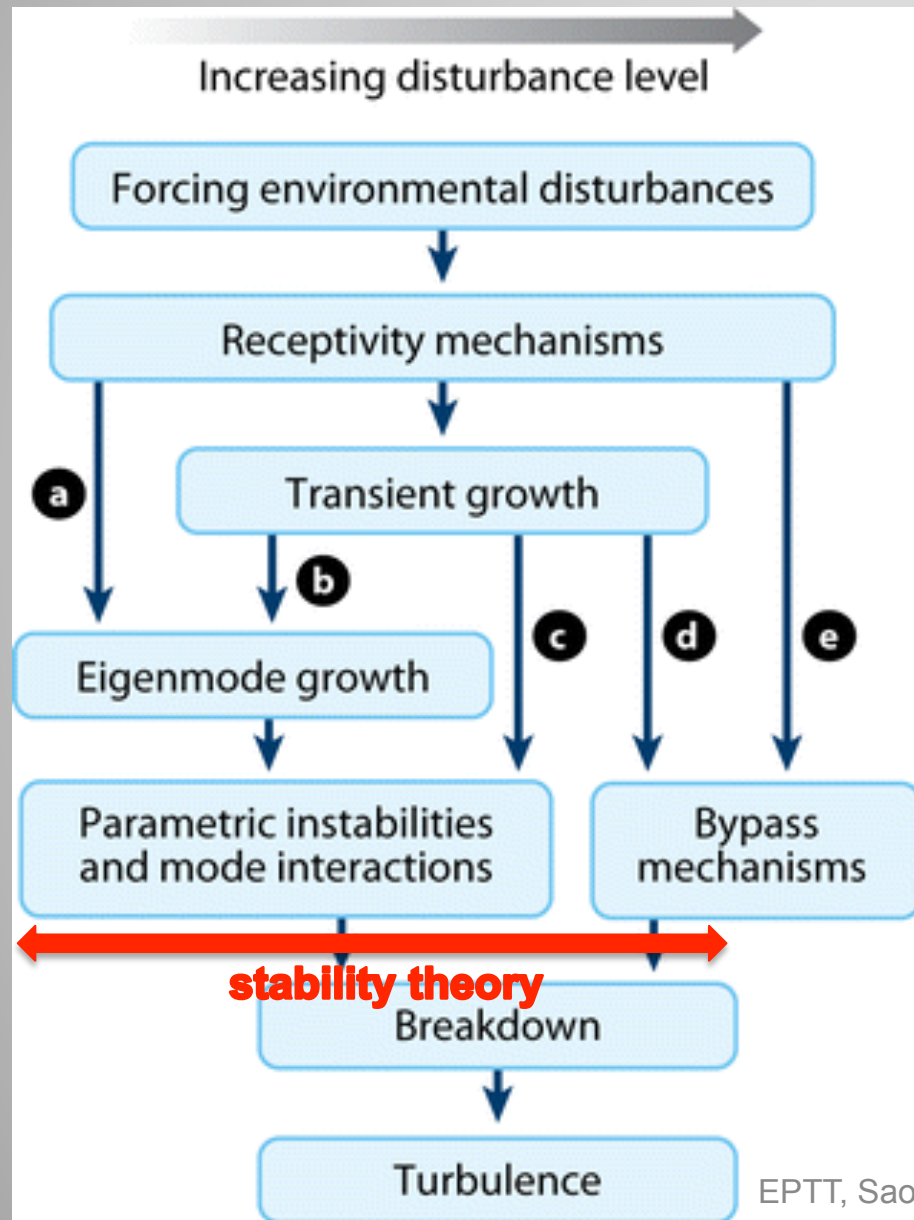
Transition to turbulence has traditionally been described by a sequence of (linear) instabilities.

Transition to turbulence



Transition to turbulence has traditionally been described by a sequence of (linear) instabilities.

Transition to turbulence: a road map



(M. Morkovin)

Stability theory is an integral part of the analysis of transition scenarios.

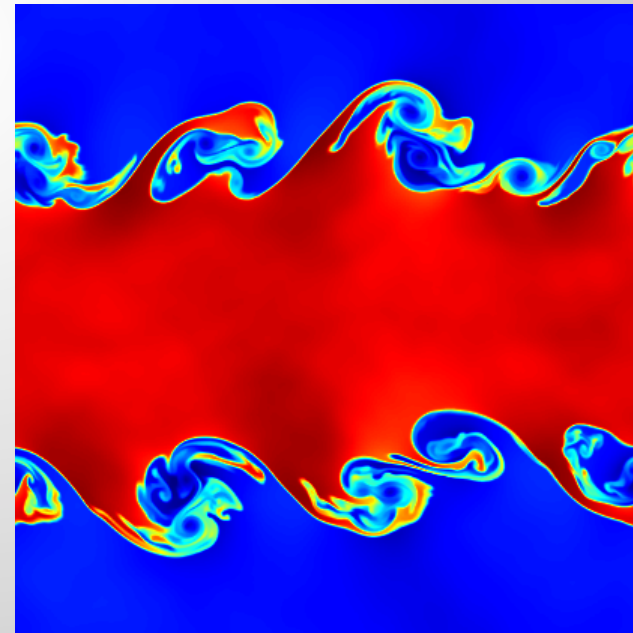
Hydrodynamic stability



Stability theory is concerned with the behavior of a fluid system with respect to a predefined base state.

Stability has to be defined carefully.

Stability is parameter-dependent.



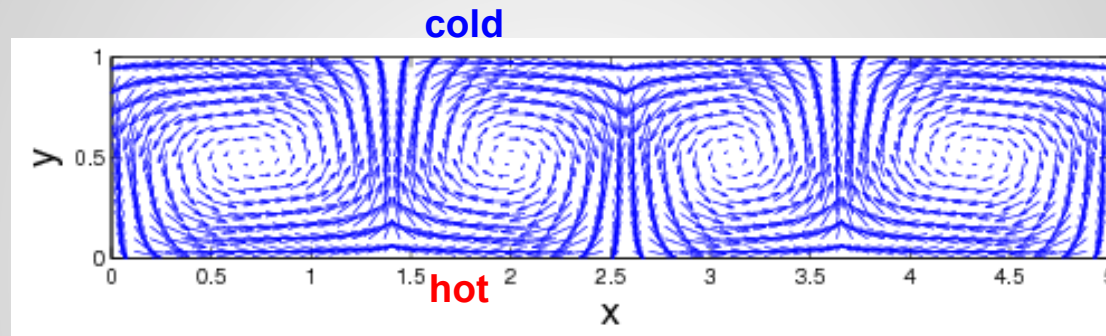
Two concepts of stability

Linear stability: we are interested in the *minimum* critical parameter above which a specific initial condition of *infinitesimal* amplitude grows *exponentially*

Energy stability: we are interested in the *maximum* critical parameter below which a general initial condition of *finite* amplitude decays *monotonically*

Two examples

Example 1: Rayleigh-Bénard convection (onset of convective instabilities can be described as an instability of the conductive state)

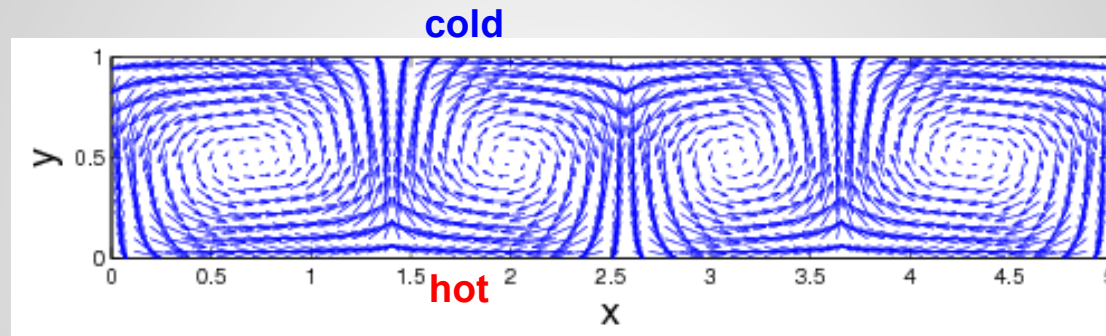


Rayleigh number (a non-dimensionalized temperature gradient) is the governing parameter

Linear stability theory: above a critical Rayleigh number of **1708** the conductive state becomes unstable to infinitesimal perturbations

Two examples

Example 1: Rayleigh-Bénard convection (onset of convective instabilities can be described as an instability of the conductive state)

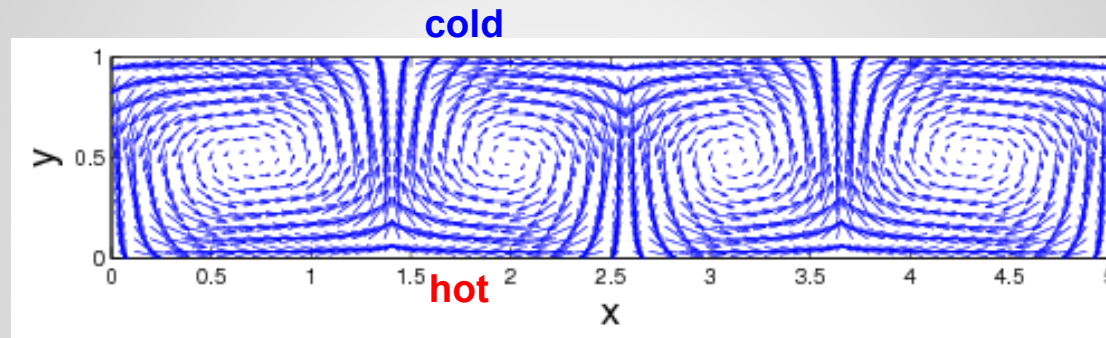


Rayleigh number (a non-dimensionalized temperature gradient) is the governing parameter

Energy stability theory: below a critical Rayleigh number of **1708** finite-amplitude perturbations superimposed on the conductive state decay monotonically in energy

Two examples

Example 1: Rayleigh-Bénard convection (onset of convective instabilities can be described as an instability of the conductive state)

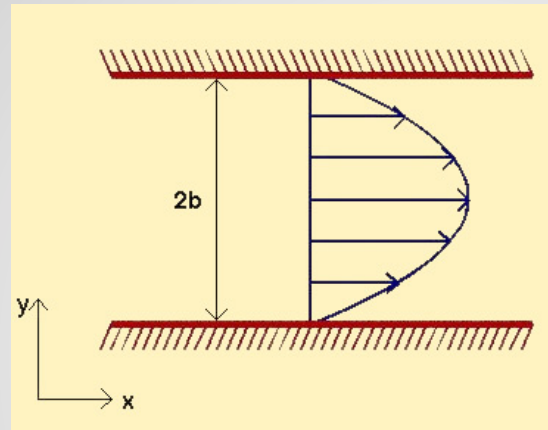


Rayleigh number (a non-dimensionalized temperature gradient) is the governing parameter

Experiments: show the onset of convective instabilities at a critical Rayleigh number of about **1710**

Two examples

Example 2: Plane Poiseuille flow (breakdown of the parabolic mean velocity profile)

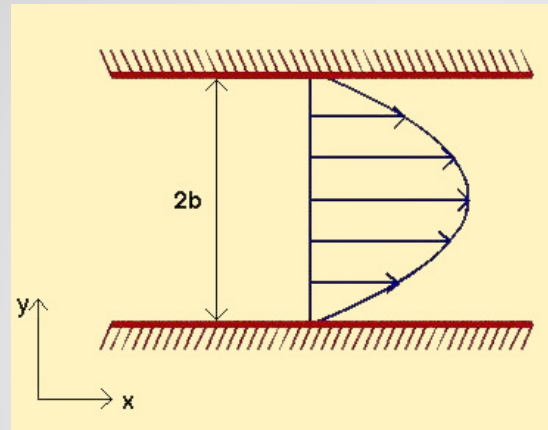


Reynolds number (a non-dimensionalized velocity) is the governing parameter

Linear stability theory: above a critical Reynolds number of **5772** the parabolic velocity profile becomes unstable to infinitesimal perturbations

Two examples

Example 2: Plane Poiseuille flow (breakdown of the parabolic mean velocity profile)

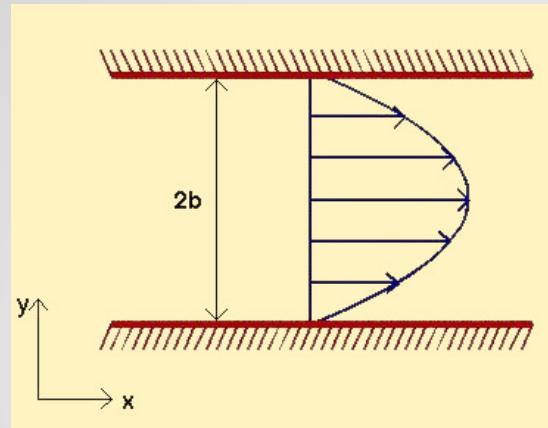


Reynolds number (a non-dimensionalized velocity) is the governing parameter

Energy stability theory: below a critical Reynolds number of **49.6** finite-amplitude perturbations superimposed on the parabolic velocity profile decay monotonically in energy

Two examples

Example 2: Plane Poiseuille flow (breakdown of the parabolic mean velocity profile)



Reynolds number (a non-dimensionalized velocity) is the governing parameter

Experiments: show the breakdown of the parabolic velocity profile at a critical Reynolds number of about **1000**

Two examples

Linear stability theory, energy stability theory and experiments are in excellent agreement for Rayleigh-Bénard convection

Linear stability theory, energy stability theory and experiments show significant discrepancies for plane Poiseuille flow

Questions:

Can we explain the success and failure of stability theory for the above two examples?

Is there a better way of investigating the stability of plane Poiseuille flow (and many other wall-bounded shear flows)?

A paradox

Fact:

The nonlinear terms in the Navier-Stokes equations conserve energy.

Fact:

During transition to turbulence we observe a substantial increase in kinetic perturbation energy, even for Reynolds numbers below the critical one.

Conclusion:

The increase in energy for subcritical Reynolds numbers has to be accomplished by a linear process, without relying on an exponential instability; i.e. we need a linear instability without an unstable eigenvalue.

Starting point are the **Navier-Stokes equations** (assuming incompressible flow)

decomposition of the flow field into mean and perturbation

$$\mathbf{u} = \mathbf{U} + \varepsilon \mathbf{u}'$$

further simplifying assumptions: uni-directional mean flow dependent on one spatial coordinate, e.g.,

$$\mathbf{U} = U(y) \hat{\mathbf{x}}$$

further simplifying assumptions: wave-like perturbation in the homogeneous directions

$$\mathbf{u} = \hat{\mathbf{u}}(y) \exp(i\alpha x + i\beta z)$$

it is convenient to eliminate the pressure (and the continuity equation) by choosing the normal velocity and normal vorticity as the dependent variables

$$\frac{\partial}{\partial t} \begin{pmatrix} \hat{v} \\ \hat{\eta} \end{pmatrix} = \begin{pmatrix} \mathcal{L}_{OS} & 0 \\ \mathcal{L}_C & \mathcal{L}_{SQ} \end{pmatrix} \begin{pmatrix} \hat{v} \\ \hat{\eta} \end{pmatrix}$$

\mathcal{L}_{OS} = Orr-Sommerfeld operator

\mathcal{L}_{SQ} = Squire operator

\mathcal{L}_C = coupling operator

Final step: discretization in the inhomogeneous direction (y) using spectral, compact- or finite-difference methods

$$\frac{d}{dt} \begin{pmatrix} v \\ \eta \end{pmatrix} = \underbrace{\begin{pmatrix} L_{OS} & 0 \\ L_C & L_{SQ} \end{pmatrix}}_L \underbrace{\begin{pmatrix} v \\ \eta \end{pmatrix}}_q$$

$$\frac{d}{dt} q = Lq$$

Formally, this equation has a solution in form of the matrix exponential of L.

$$\frac{d}{dt}q = Lq$$

$$q = \exp(tL)q_0$$

$$q_0 = q(t = 0)$$

The matrix exponential of L is the stability operator after the linearization step.

$$q = \exp(tL)q_0$$

We can redefine the concept of stability based on the matrix exponential by considering the growth of perturbation energy over time.

$$G(t) = \max_{q_0} \frac{\|q\|^2}{\|q_0\|^2} = \max_{q_0} \frac{\|\exp(tL)q_0\|^2}{\|q_0\|^2}$$

$G(t)$ represents the amplification of perturbation energy maximized over all initial conditions.

$$q = \exp(tL)q_0$$

We can redefine the concept of stability based on the matrix exponential by considering the growth of perturbation energy over time.

$$G(t) = \max_{q_0} \frac{\|q\|^2}{\|q_0\|^2} = \|\exp(tL)\|^2$$

$G(t)$ represents the amplification of perturbation energy maximized over all initial conditions.

In general, the matrix exponential is difficult to compute. In its place, eigenvalues of L have been used as proxies.

$$L = S\Lambda S^{-1} \quad \text{eigenvalue decomposition}$$

$$\|\exp(tL)\|^2 = \|\exp(tS\Lambda S^{-1})\|^2 = \|S \exp(t\Lambda) S^{-1}\|^2$$

traditional stability analysis



In traditional stability analysis, the behavior of $G(t)$ is deduced from the eigenvalues of L .

Do the eigenvalues of L capture the behavior of $G(t)$?

We can answer this question by computing upper and lower bounds (estimates) on $G(t)$.

The energy cannot decay at a faster rate than the one given by the least stable eigenvalue λ_{\max}

lower bound
$$e^{2t\lambda_{\max}} \leq \|\exp(tL)\|^2$$

For the upper bound we use the eigenvalue decomposition of L .

upper bound
$$\begin{aligned} \|\exp(tL)\|^2 &= \|S \exp(t\Lambda) S^{-1}\|^2 \\ &\leq \|S\|^2 \|S^{-1}\|^2 e^{2t\lambda_{\max}} \end{aligned}$$

We can answer this question by computing upper and lower bounds (estimates) on $G(t)$.

$$e^{2t\lambda_{\max}} \leq \|\exp(tL)\|^2 \leq \boxed{\|S\|^2 \|S^{-1}\|^2} e^{2t\lambda_{\max}}$$

1

Two cases can be distinguished:

$$\kappa(S) = \|S\|^2 \|S^{-1}\|^2 = 1$$

upper and lower bound coincide: the energy amplification is governed by the least stable eigenvalue

We can answer this question by computing upper and lower bounds (estimates) on $G(t)$.

$$e^{2t\lambda_{\max}} \leq \|\exp(tL)\|^2 \leq \boxed{\|S\|^2 \|S^{-1}\|^2} e^{2t\lambda_{\max}} \gg 1$$

Two cases can be distinguished:

$$\kappa(S) = \|S\|^2 \|S^{-1}\|^2 \gg 1$$

upper and lower bound can differ significantly:
the energy amplification is governed by the least stable eigenvalue **only for large times**

This suggests distinguishing two different classes of stability problems.

$$\kappa(S) = \|S\|^2 \|S^{-1}\|^2 = 1 \quad \text{normal stability problems}$$

- orthogonal eigenvectors
- eigenvalue analysis captures the dynamics

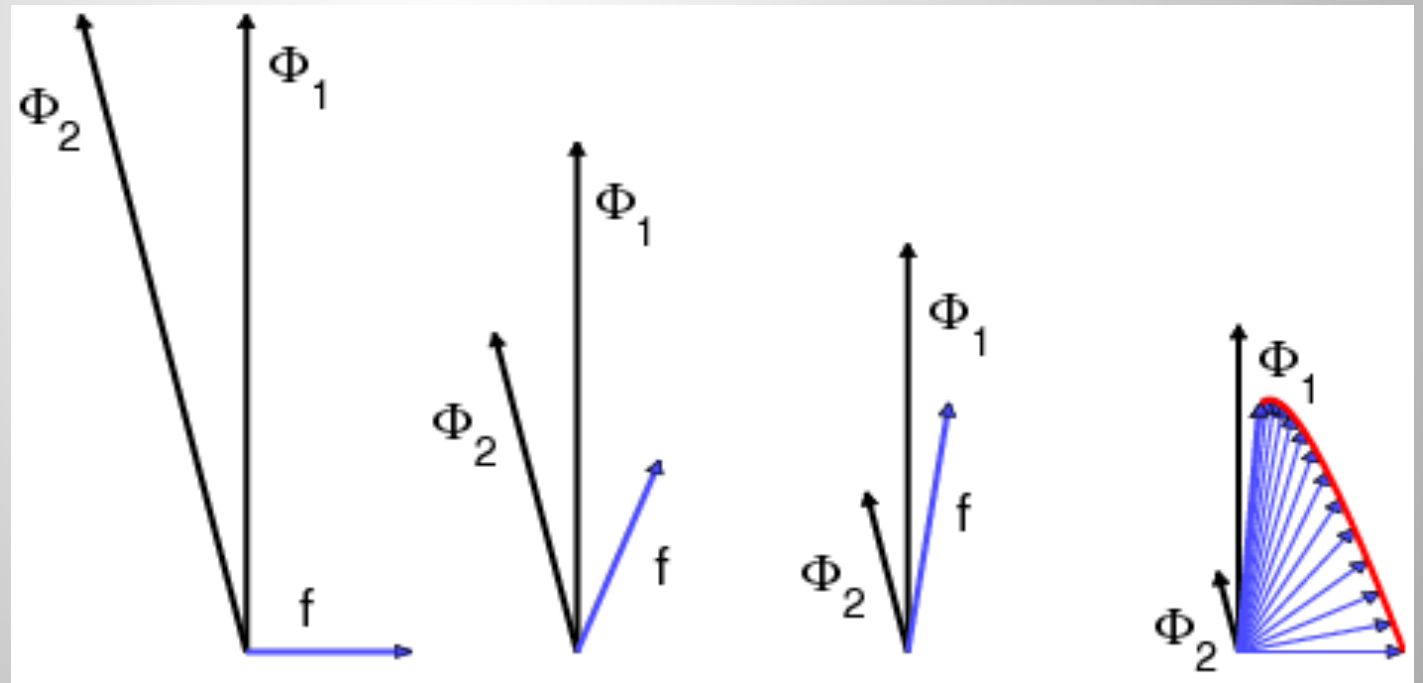
$$\kappa(S) = \|S\|^2 \|S^{-1}\|^2 \gg 1 \quad \text{nonnormal stability problems}$$

- non-orthogonal eigenvectors
- eigenvalue analysis captures the asymptotic dynamics, but not the short-time behavior

The nonnormality of the system can give rise to transient energy amplification.

Even though we experience exponential decay for large times, the non-orthogonal superposition of eigenvectors can lead to short-time growth of energy.

Geometric interpretation:



Is there a better way of describing the short-time dynamics of nonnormal stability problems ?

$$\kappa(S) = \|S\|^2 \|S^{-1}\|^2 \gg 1$$

We start with a Taylor expansion of the matrix exponential about $t=0$.

$$\begin{aligned} E(t) &= \langle q, q \rangle = \|q\|^2 \\ &= \langle \exp(tL)q_0, \exp(tL)q_0 \rangle \\ &\approx \langle (I + tL)q_0, (I + tL)q_0 \rangle \\ &\approx \langle q_0, q_0 \rangle + t \langle q_0, (L + L^H)q_0 \rangle \end{aligned}$$

$$E(t) \approx \langle q_0, q_0 \rangle + t \langle q_0, (L + L^H)q_0 \rangle$$

The initial energy growth rate is given by

$$\frac{1}{E} \frac{dE}{dt} \Big|_{t=0^+} = \frac{\langle q_0, (L + L^H)q_0 \rangle}{\langle q_0, q_0 \rangle}$$

$(L + L^H)$ is Hermitian (symmetric)

$$\frac{1}{E} \frac{dE}{dt} \Big|_{t=0^+} = \lambda_{\max}(L + L^H)$$

numerical abscissa of L

The numerical abscissa can be generalized to the **numerical range**.

$$\begin{aligned}\frac{d}{dt} \|q\|^2 &= \left\langle \frac{d}{dt} q, q \right\rangle + \left\langle q, \frac{d}{dt} q \right\rangle \\ &= \langle Lq, q \rangle + \langle q, Lq \rangle \\ &= 2\text{Real} \{ \langle Lq, q \rangle \}\end{aligned}$$

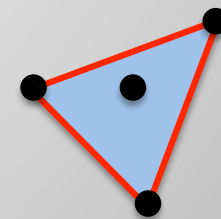
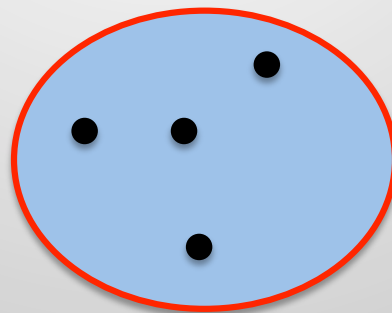
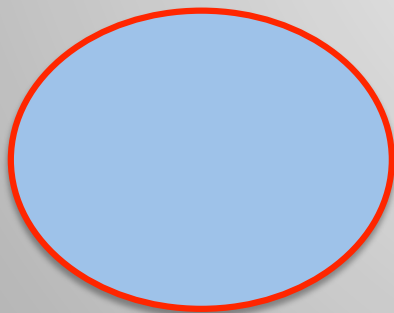
Definition of the numerical range:

$$\mathcal{F}(L) = \left\{ z \mid z = \frac{\langle Lq, q \rangle}{\langle q, q \rangle} \right\} \quad \text{set of all Rayleigh quotients of } L$$

$$\mathcal{F}(L) = \left\{ z \mid z = \frac{\langle Lq, q \rangle}{\langle q, q \rangle} \right\} \quad \text{set of all Rayleigh quotients of } L$$

Three important properties of the numerical range:

1. The numerical range is convex.
2. The numerical range contains the spectrum of L .
3. For normal L , the numerical range is the convex hull of the spectrum.



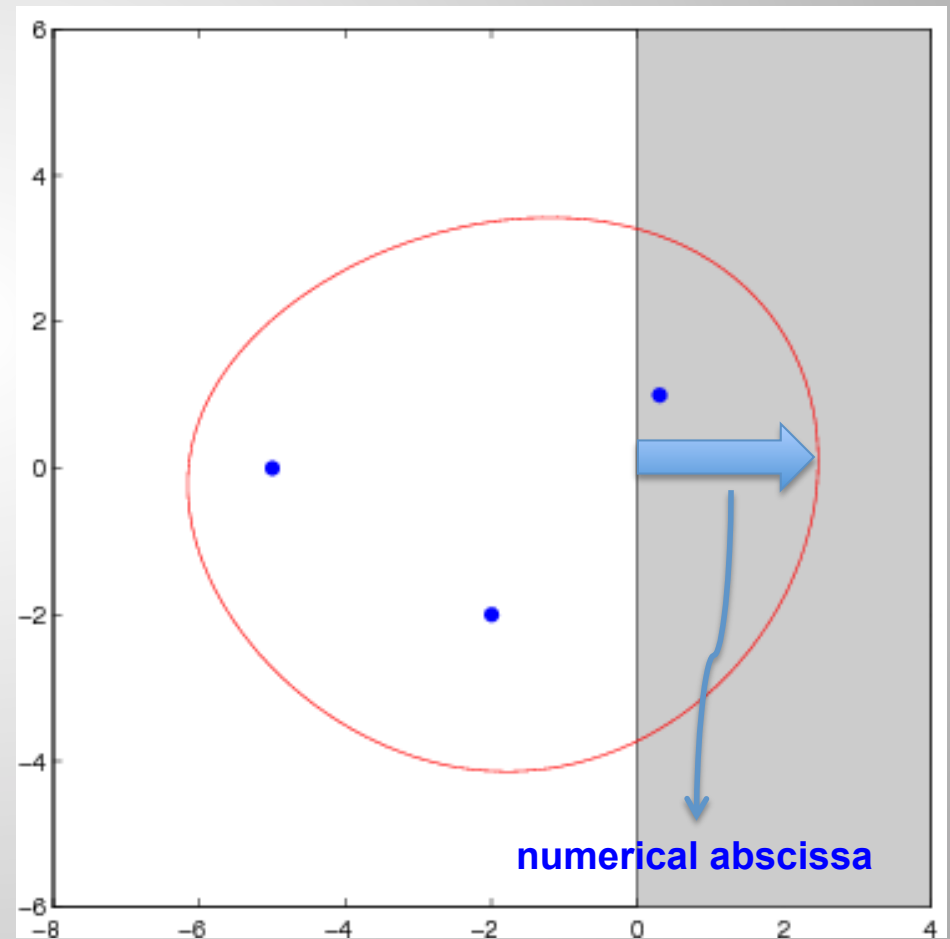
$$\mathcal{F}(L) = \left\{ z \mid z = \frac{\langle Lq, q \rangle}{\langle q, q \rangle} \right\}$$

set of all Rayleigh quotients of L

Illustration:

$$A = \begin{pmatrix} -5 & 4 & 4 \\ & -2 - 2i & 4 \\ & & 0.3 + i \end{pmatrix}$$

The numerical range is substantially larger than the convex hull of the spectrum.



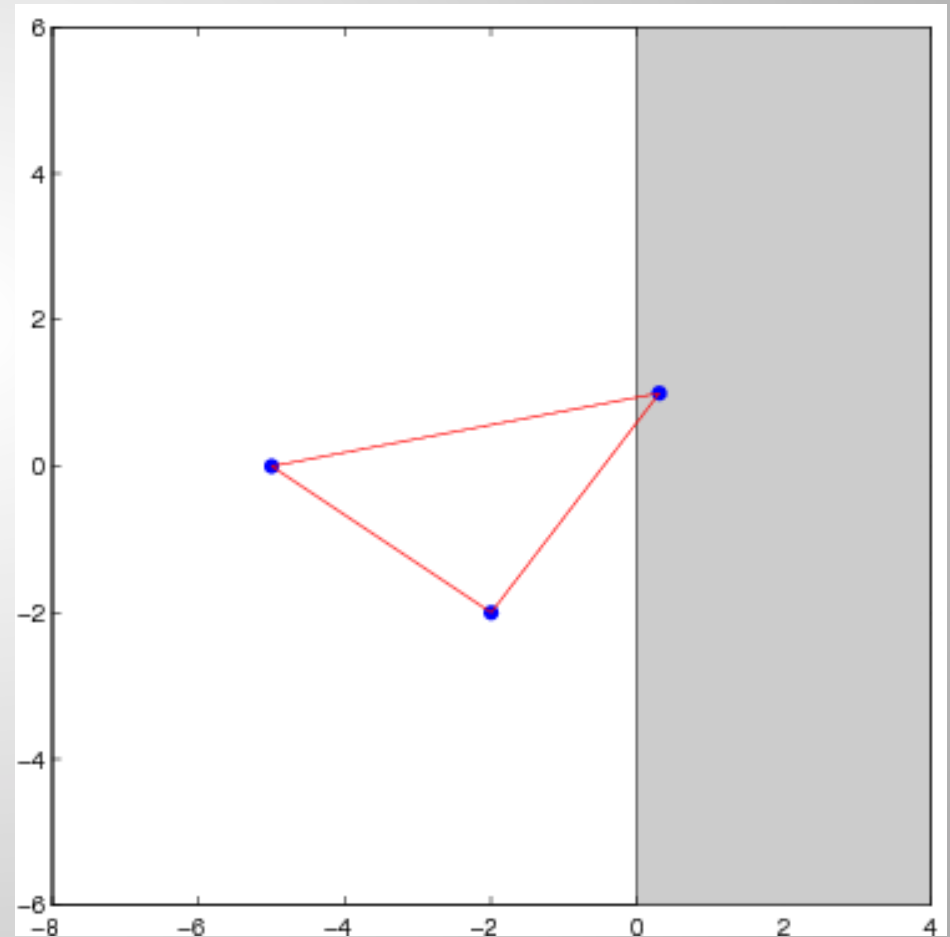
$$\mathcal{F}(L) = \left\{ z \mid z = \frac{\langle Lq, q \rangle}{\langle q, q \rangle} \right\}$$

set of all Rayleigh quotients of L

Illustration:

$$A = \begin{pmatrix} -5 & & \\ & -2 - 2i & \\ & & 0.3 + i \end{pmatrix}$$

The numerical range is the convex hull of the spectrum.



For nonnormal stability problems:

The numerical abscissa (numerical range) governs the very short time behavior. The sign of the numerical abscissa determines initial energy growth or decay.

The least stable eigenvalue governs the long time behavior. The sign of the real part of λ_{\max} determines asymptotic energy growth or decay.



revisit Rayleigh-Bénard convection and plane Poiseuille flow

Rayleigh-Bénard convection is a normal stability problem



The numerical range is the convex hull of the spectrum.



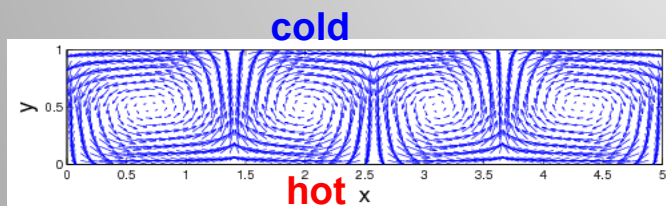
The numerical range and the spectrum cross into the unstable half-plane at the same Rayleigh number.



Initial energy growth and asymptotic instability occur at the same Rayleigh number.



$$Ra_{lin} = Ra_{ener} = 1708$$



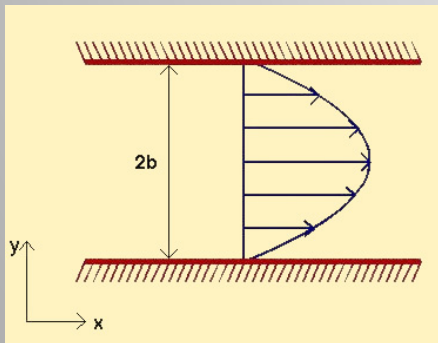
The spectrum governs the perturbation dynamics at all times.

plane Poiseuille flow is a nonnormal stability problem

↪ The numerical range is larger than the convex hull of the spectrum.

↪ The numerical range crosses into the unstable half-plane « before » the spectrum crosses into the unstable half-plane.

↪ Initial energy growth is possible « before » asymptotic instability occurs.



↪ $Re_{lin} = 5772 \gg Re_{ener} = 49.6$

↪ The spectrum governs the perturbation dynamics only in the asymptotic limit of $t \rightarrow \infty$

Summary

short time

$$\frac{1}{E} \frac{dE}{dt} \Big|_{t=0+} = \lambda_{\max}(L + L^H)$$

(numerical abscissa)

all time

$$\| \exp(tL) \|^2$$

(matrix exponential norm)


long time

$$G(t \rightarrow \infty) = \lim_{t \rightarrow \infty} \| \exp(tL) \| = e^{t\lambda_{\max}}$$

(eigenvalues)

The energy amplification curve $G(t)$ is the envelope over many individual growth curves.

For each point on this curve, a specific initial condition reaches its maximum energy amplification at this point (in time).

Can we recover the initial condition that results in the maximum energy amplification at a given time?  optimal initial condition

equation that governs the optimal initial condition

$$\exp(t^* L) q_0 = q(t^*)$$

q_0 input (initial condition)
 $q(t^*)$ output (final condition)

Assume that the initial condition satisfies $\|q_0\| = 1$ and normalize the output such that $\|\bar{q}(t^*)\| = 1$

$$\exp(t^* L) \bar{q}_0 = \|\exp(t^* L)\| \bar{q}(t^*)$$

propagator input amplification output

$$\underbrace{\exp(t^* L)}_{\text{propagator}} \underbrace{\bar{q}_0}_{\text{input}} = \underbrace{\|\exp(t^* L)\|}_{\text{amplification}} \underbrace{\bar{q}(t^*)}_{\text{output}}$$

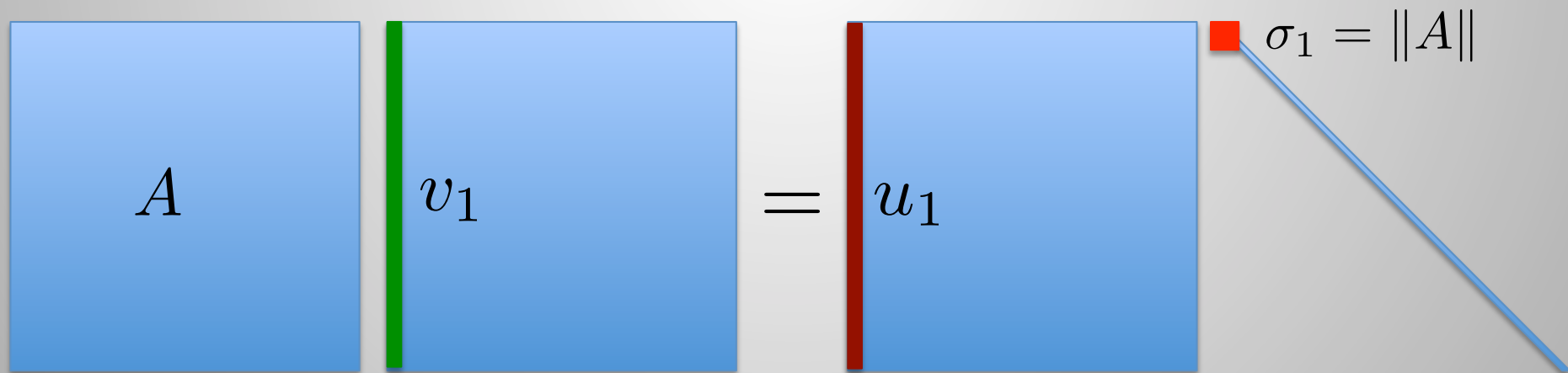
The singular-value decomposition of a matrix A is

$$A = \underbrace{U}_{\substack{\text{unitary} \\ \text{(orthogonal)}}} \underbrace{\Sigma}_{\text{diagonal}} \underbrace{V^H}_{\substack{\text{unitary} \\ \text{(orthogonal)}}$$

$$\underbrace{\exp(t^* L)}_{\text{propagator}} \underbrace{\bar{q}_0}_{\text{input}} = \underbrace{\|\exp(t^* L)\|}_{\text{amplification}} \underbrace{\bar{q}(t^*)}_{\text{output}}$$

The singular-value decomposition of a matrix A is

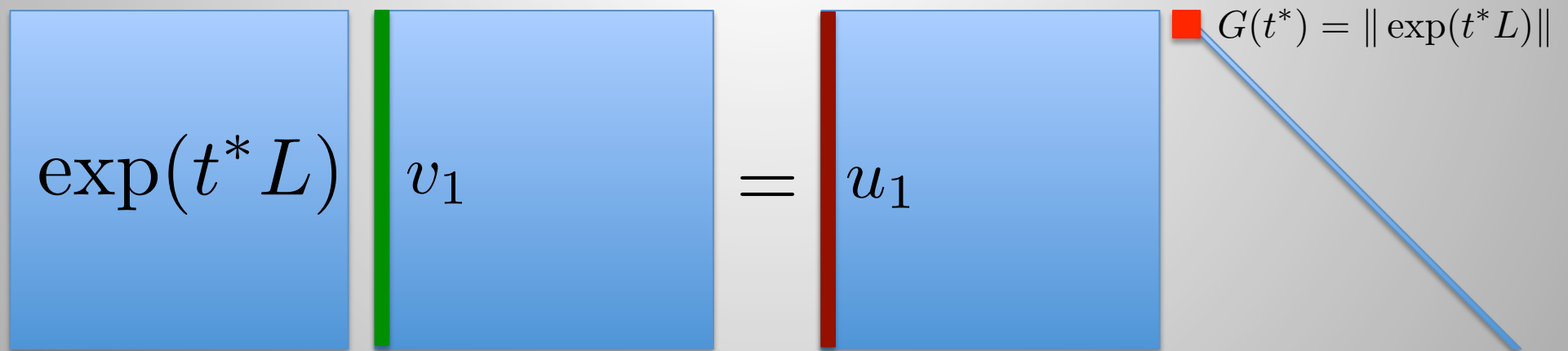
$$AV = U\Sigma$$



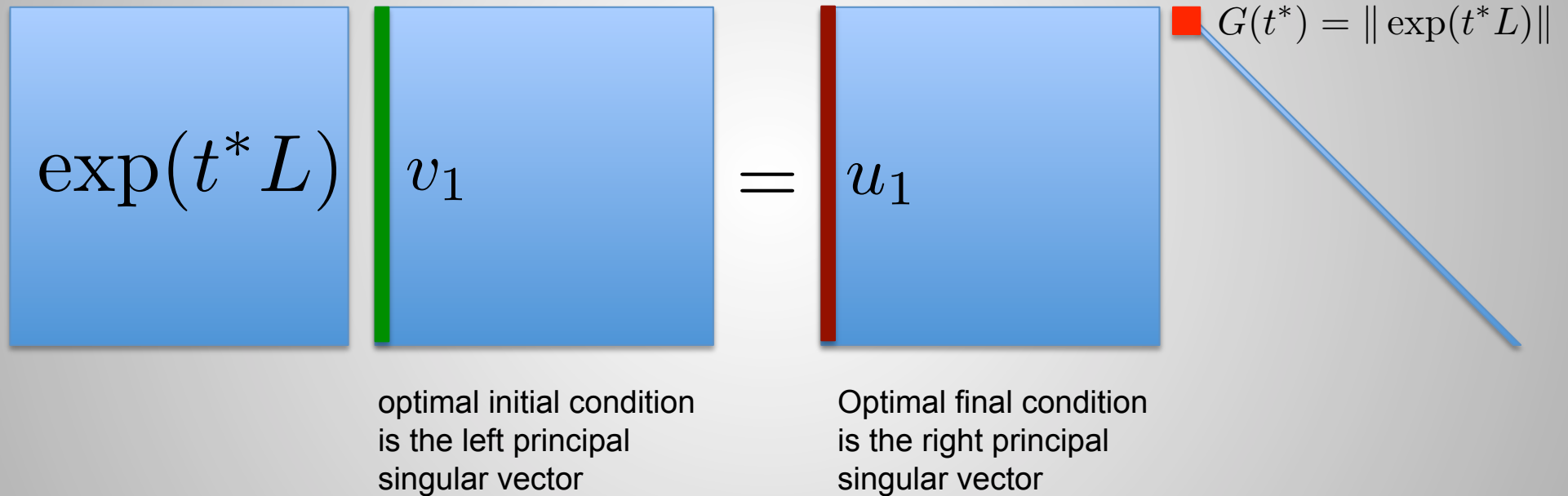
$$\underbrace{\exp(t^* L)}_{\text{propagator}} \underbrace{\bar{q}_0}_{\text{input}} = \underbrace{\|\exp(t^* L)\|}_{\text{amplification}} \underbrace{\bar{q}(t^*)}_{\text{output}}$$

The singular-value decomposition of our matrix exponential at t^* is

$$\text{svd}(\exp(t^* L)) = U \Sigma V^H$$



$$\underbrace{\exp(t^* L)}_{\text{propagator}} \underbrace{\bar{q}_0}_{\text{input}} = \underbrace{\|\exp(t^* L)\|}_{\text{amplification}} \underbrace{\bar{q}(t^*)}_{\text{output}}$$



often we are interested in the response of our fluid system to external forces (modelling free-stream turbulence, acoustic waves, wall-roughness etc.)

in this case, our governing equation can be formulated as

$$\frac{d}{dt}q = Lq + f \quad f \text{ model of external forces}$$

the response to forcing (particular solution, i.e., zero initial condition) is

$$q_p = \int_0^t \exp((\tau - t)L) f(\tau) d\tau$$

(memory integral)

for the special case of harmonic forcing $f = \hat{f}e^{i\omega t}$

this simplifies to

$$\hat{q}_p = (i\omega - L)^{-1} \hat{f}$$

and the optimal response (optimized over all possible forcing functions) becomes

$$R(\omega) = \max_{\hat{f}} \frac{\|\hat{q}_p\|}{\|\hat{f}\|} = \max_{\hat{f}} \frac{\|(i\omega - L)^{-1} \hat{f}\|}{\|\hat{f}\|} = \|(i\omega - L)^{-1}\|$$

(resolvent norm)

eigenvalue-based analysis recovers the classical resonance condition

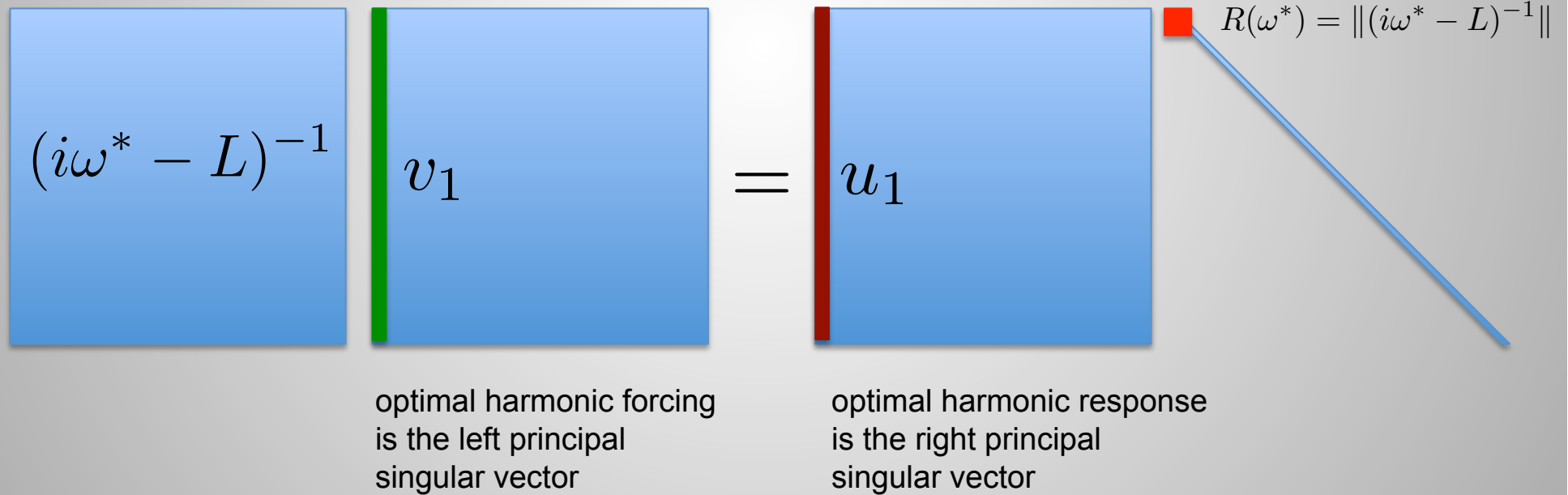
$$\|(i\omega - L)^{-1}\| = \|S(i\omega - \Lambda)^{-1}S^{-1}\| \leq \kappa(S) \frac{1}{\text{dist}\{i\omega, \Lambda\}}$$

for a **normal** system, the classical resonance condition (closeness of forcing frequency to one of the eigenfrequencies) holds

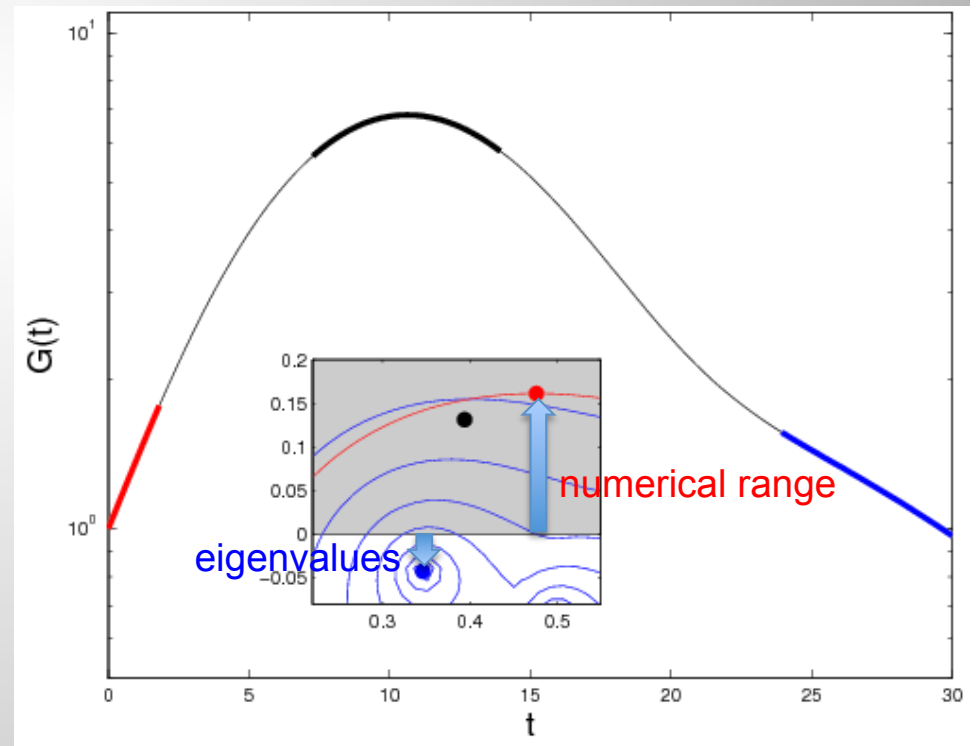
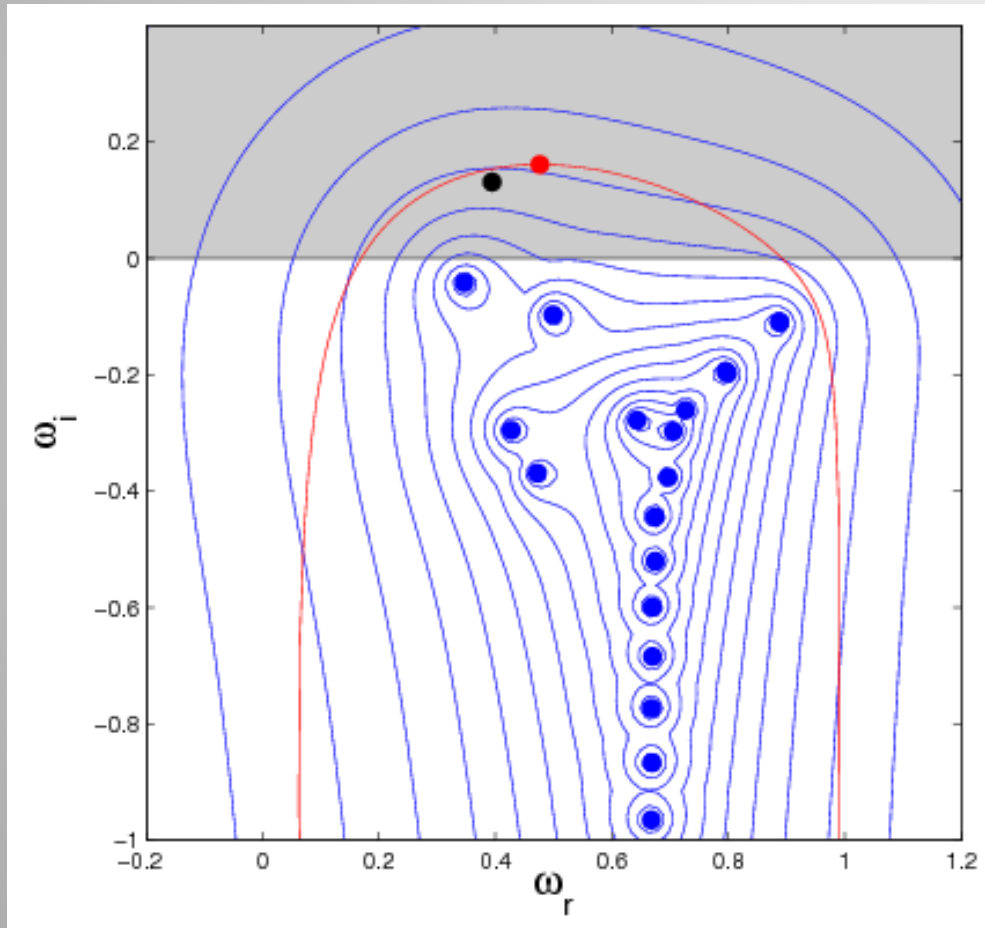
for a **non-normal** system, we can have a **pseudo-resonance** (large response to outside forcing) even though the forcing frequency is far from an eigenfrequency of the linear system

to obtain the optimal forcing we proceed as before (i.e., take the svd)

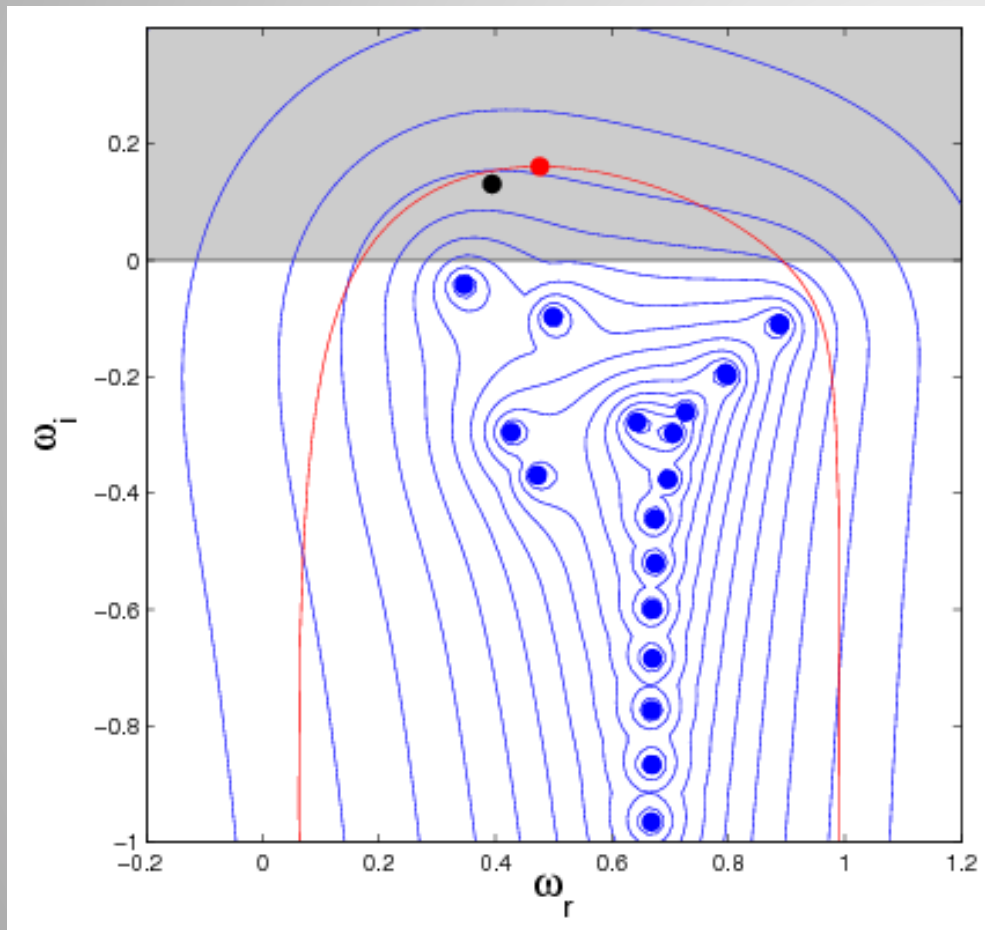
$$\underbrace{(i\omega^* - L)^{-1}}_{\text{transfer function}} \underbrace{\bar{f}}_{\text{forcing (unit energy)}} = \underbrace{\| (i\omega^* - L)^{-1} \|}_{\text{amplification}} \underbrace{\bar{q}_p}_{\text{response (unit energy)}}$$



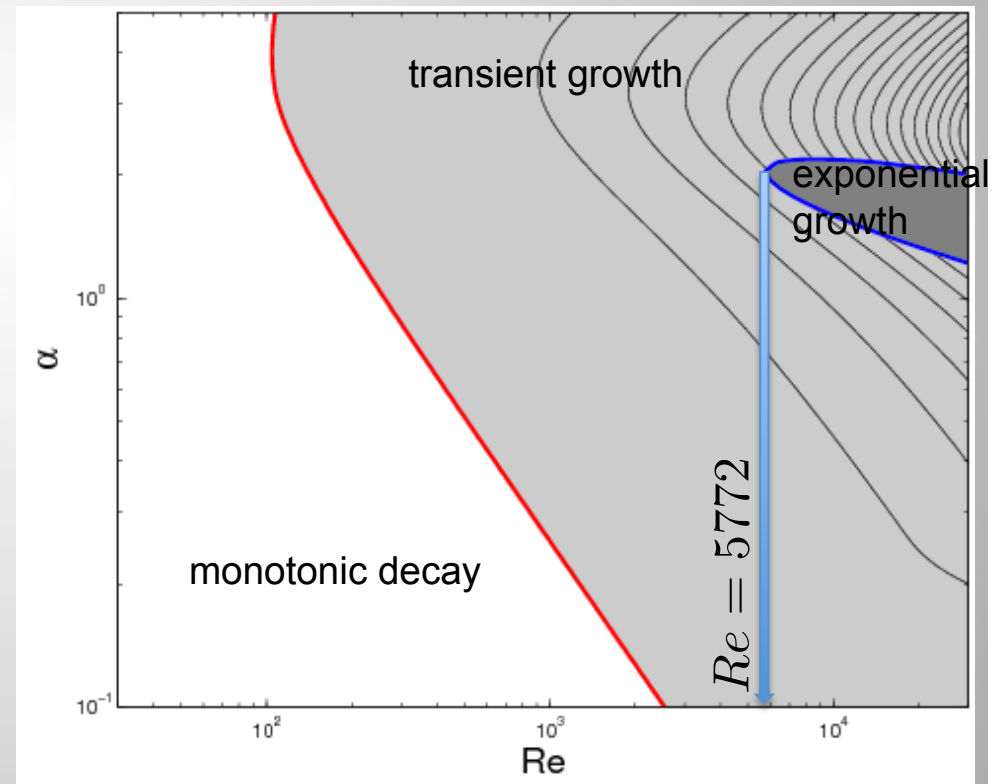
Example: plane Poiseuille flow



Example: plane Poiseuille flow

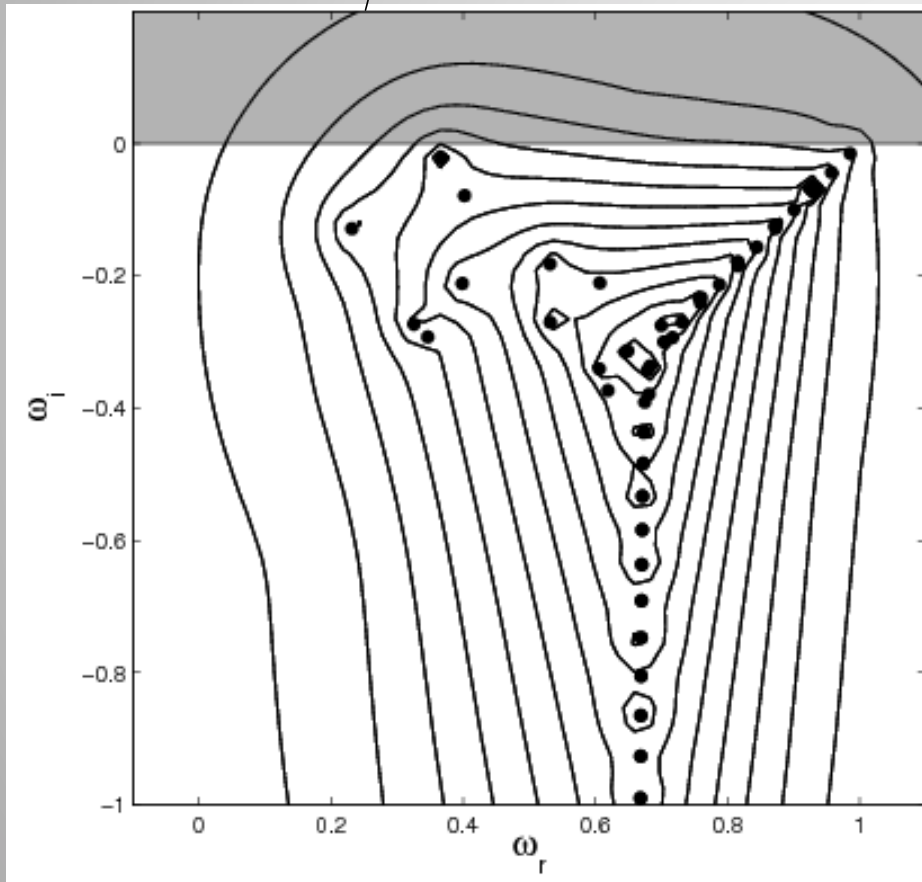


neutral curve

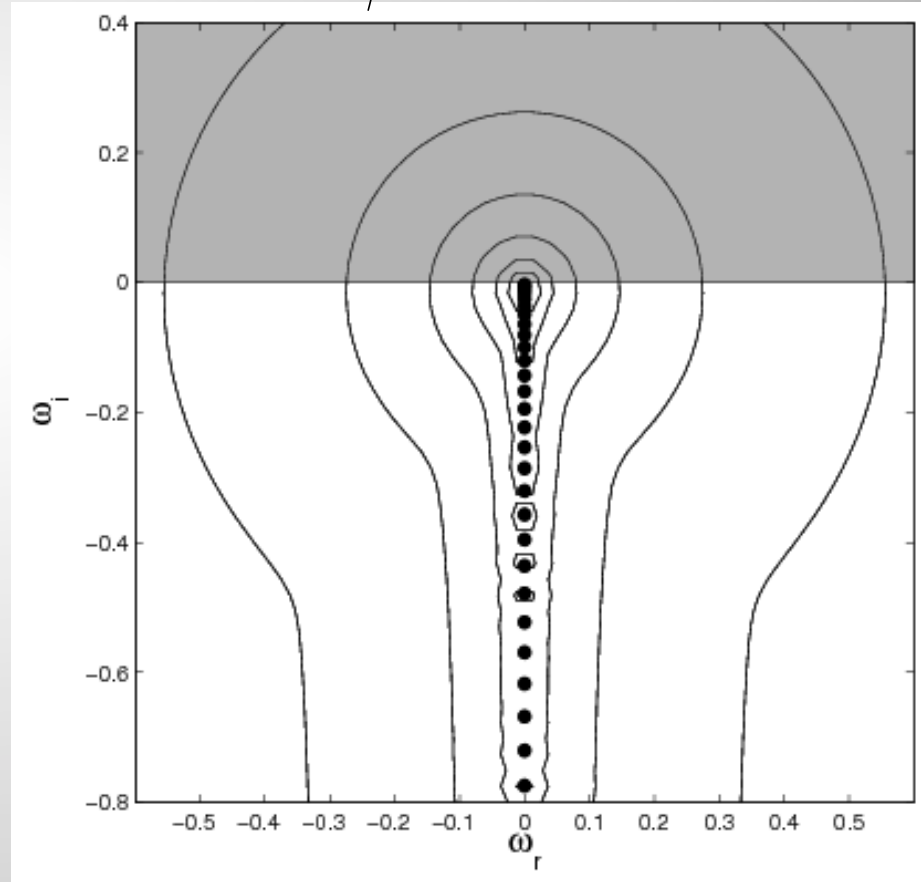


Example: plane Poiseuille flow

$\alpha = 1 \quad \beta = 1 \quad Re = 2500$

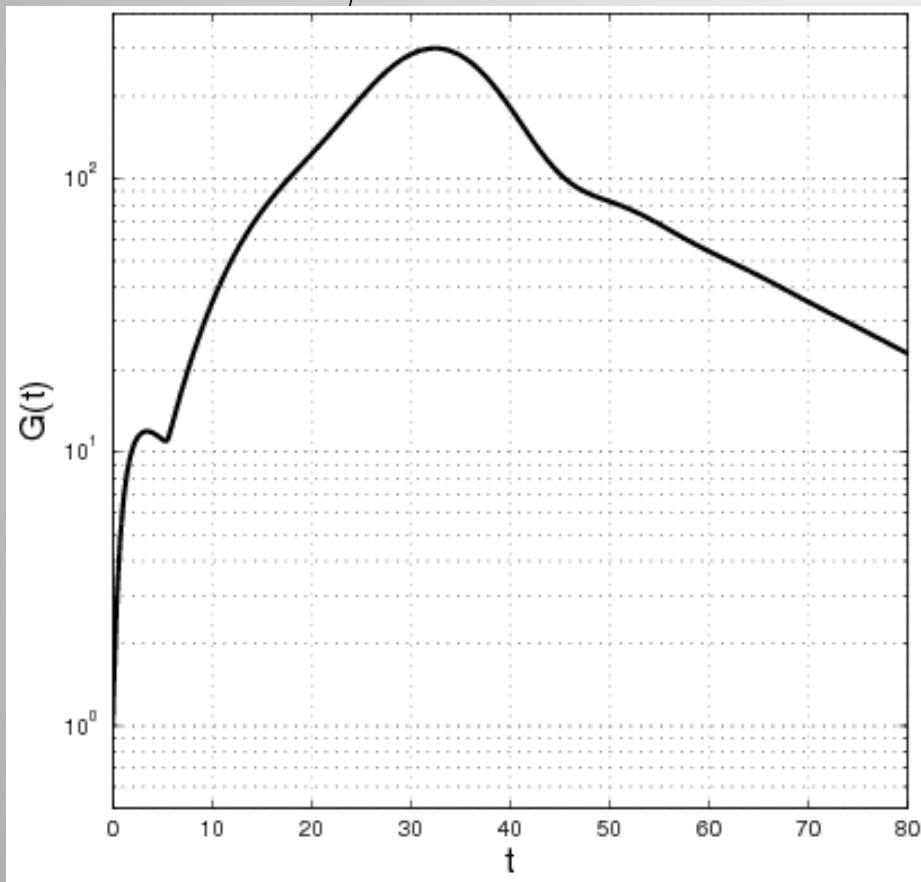


$\alpha = 0 \quad \beta = 2 \quad Re = 2500$

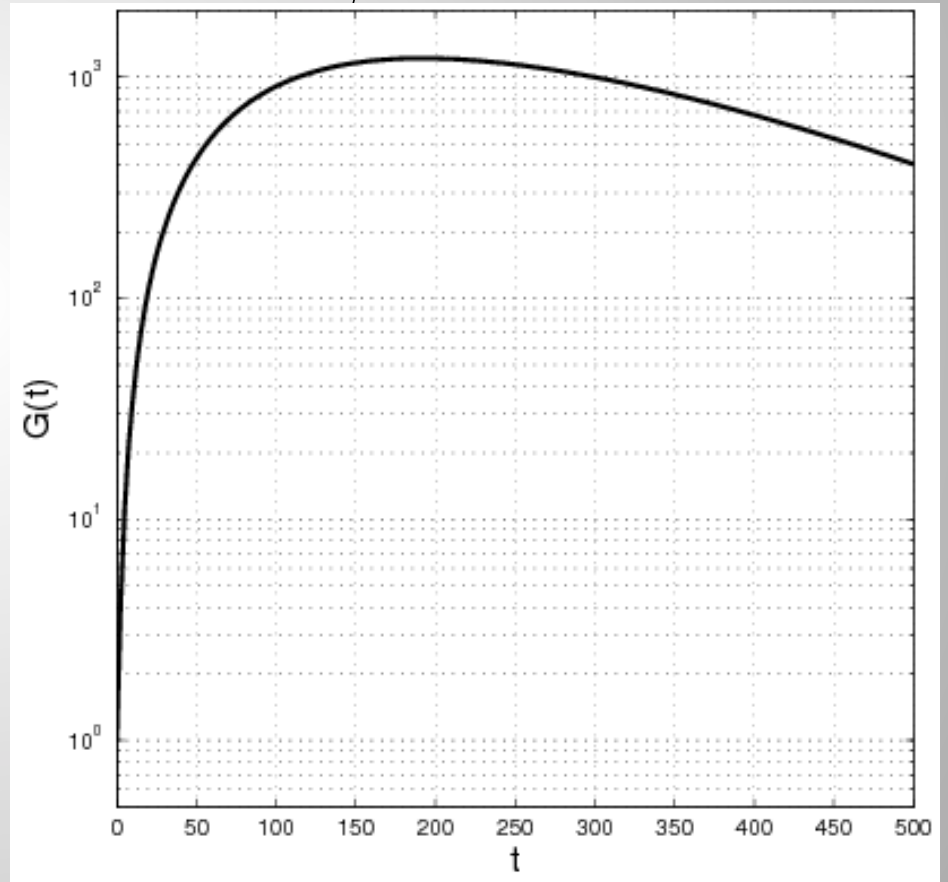


Example: plane Poiseuille flow

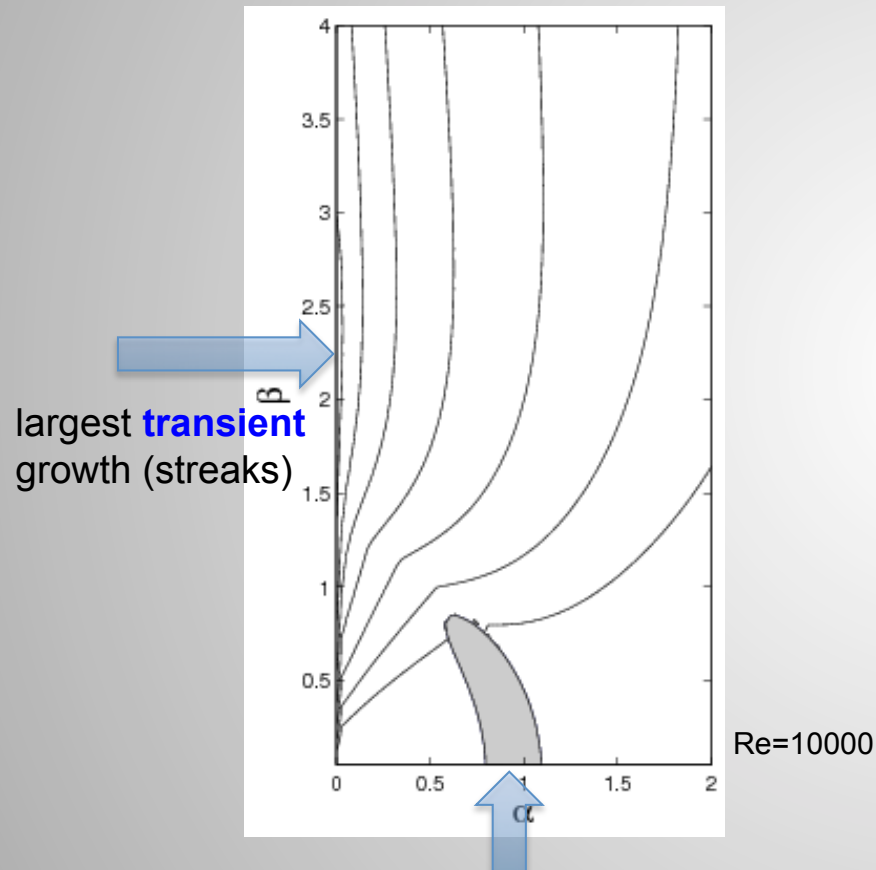
$$\alpha = 1 \quad \beta = 1 \quad Re = 2500$$



$$\alpha = 0 \quad \beta = 2 \quad Re = 2500$$



Example: plane Poiseuille flow

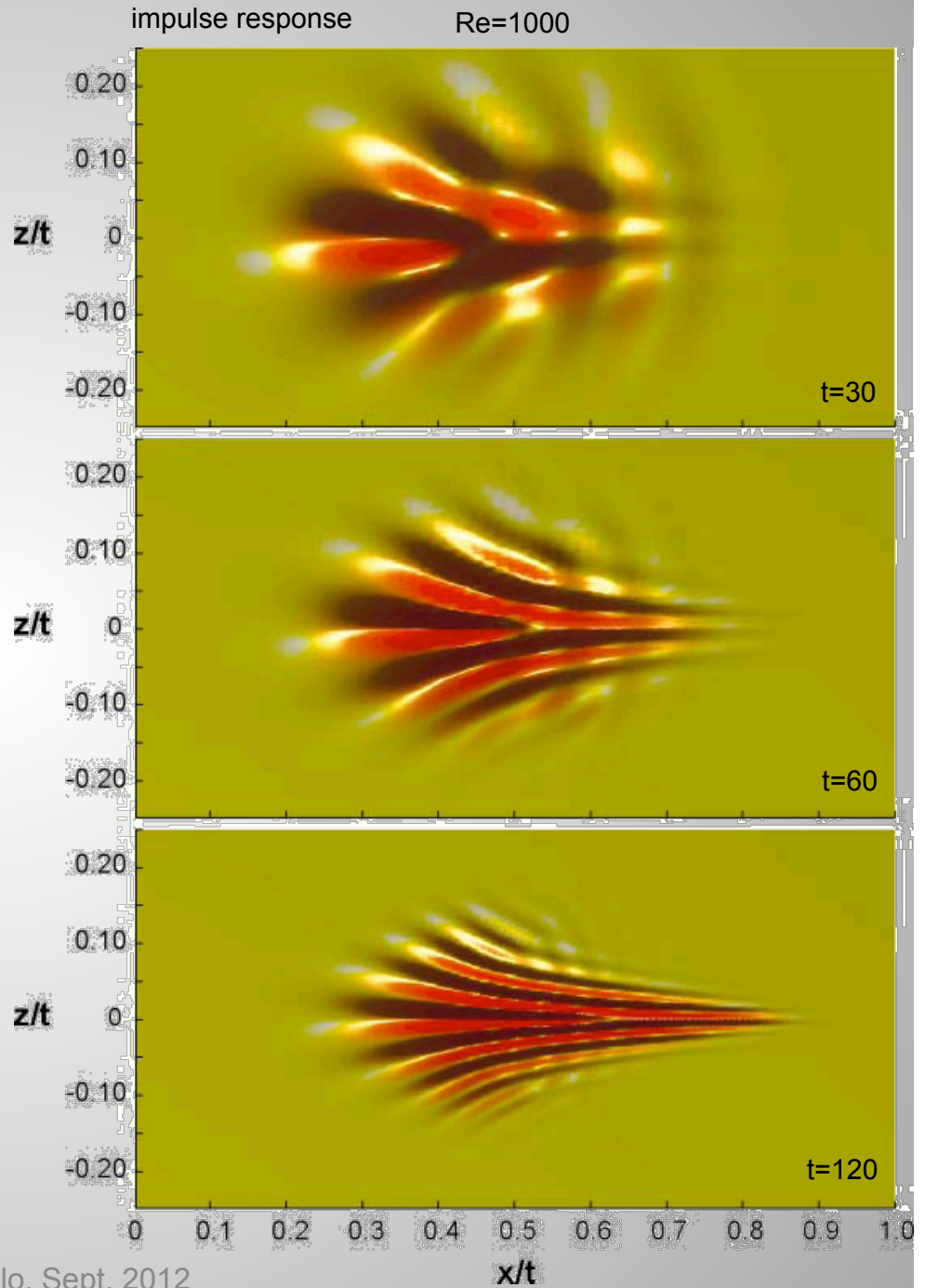
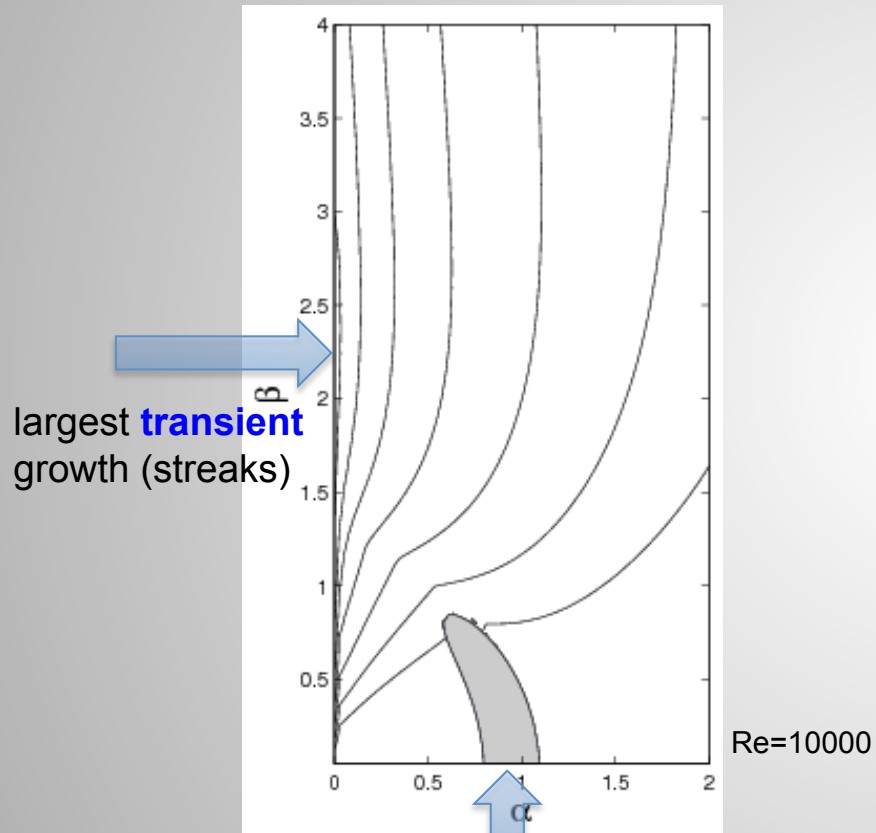


Over a short time-horizon, structures with no or weak *streamwise* dependence are favored.

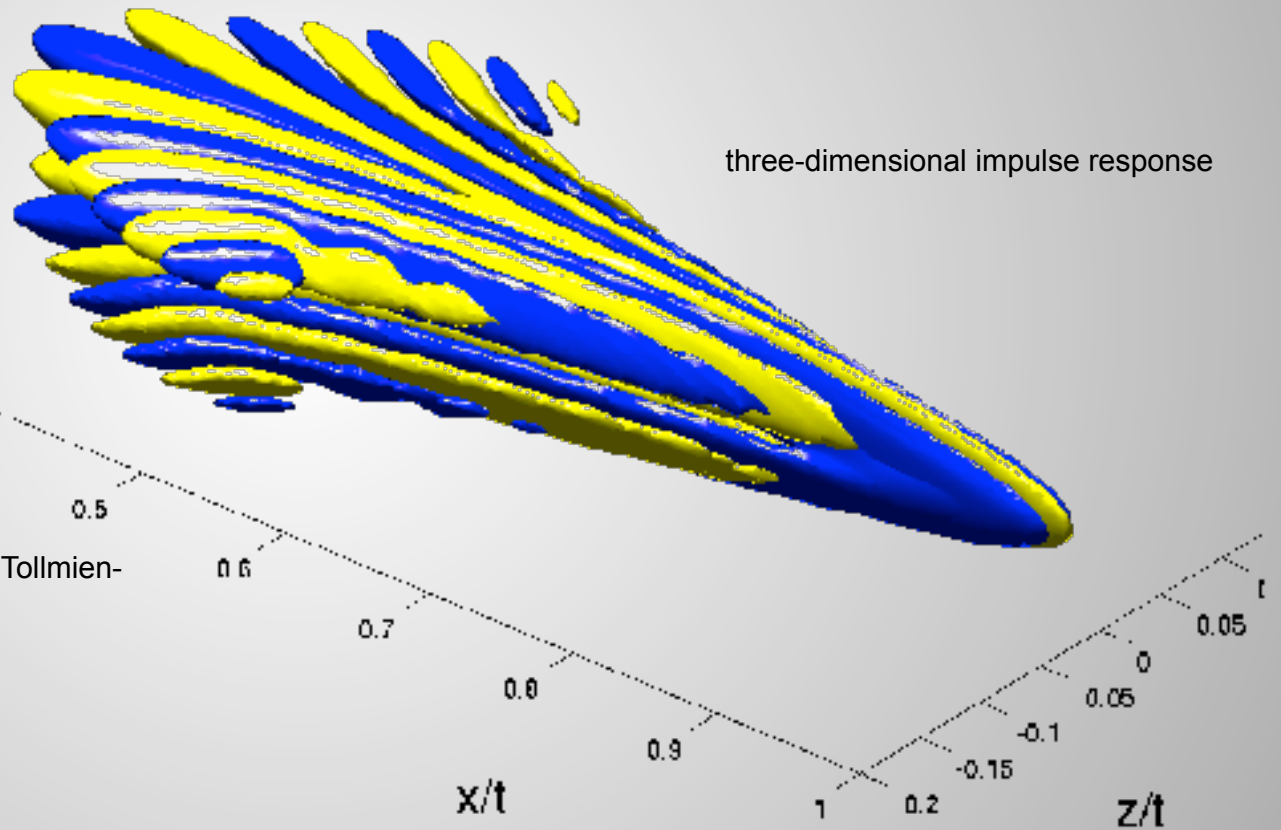
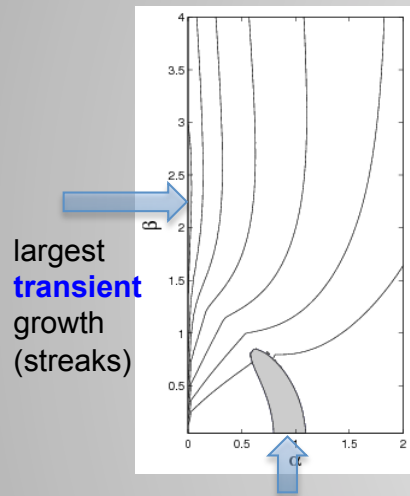
Over a very long (infinite) time-horizon, structures with no or weak *spanwise* dependence are favored.

largest **exponential** growth
(Tollmien-Schlichting wave)

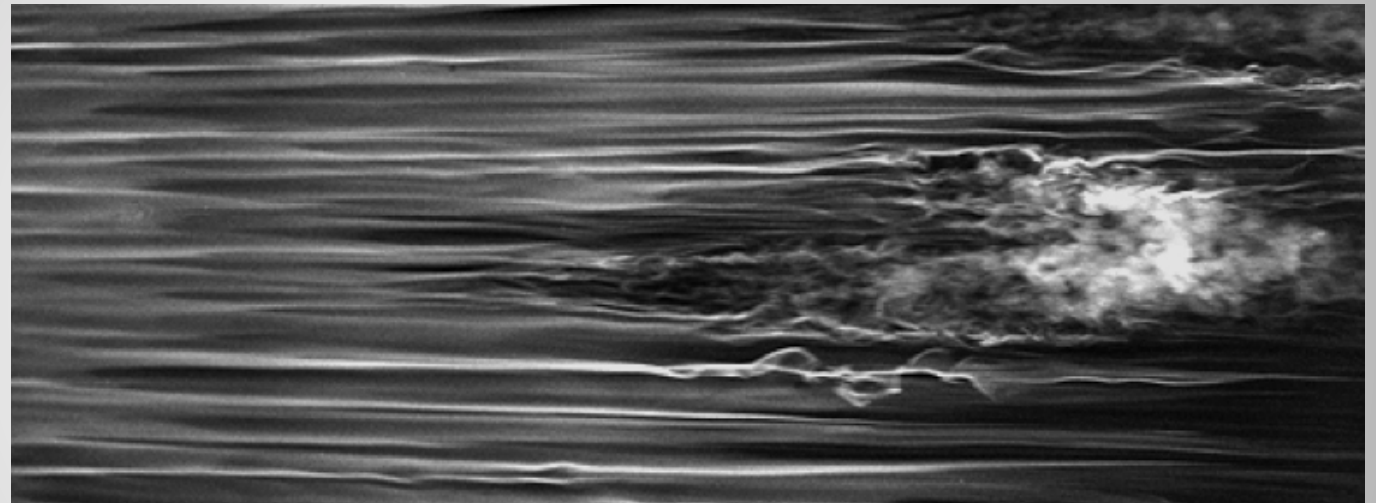
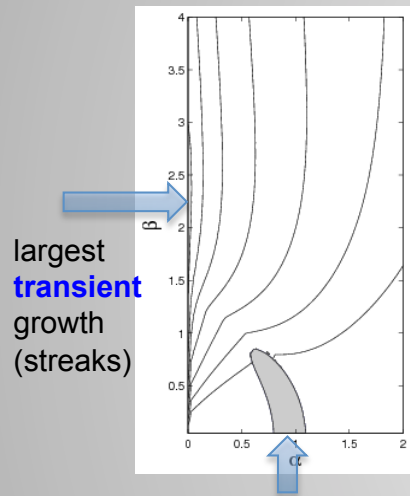
Example: plane Poiseuille flow



Example: plane Poiseuille flow



Example: plane Poiseuille flow



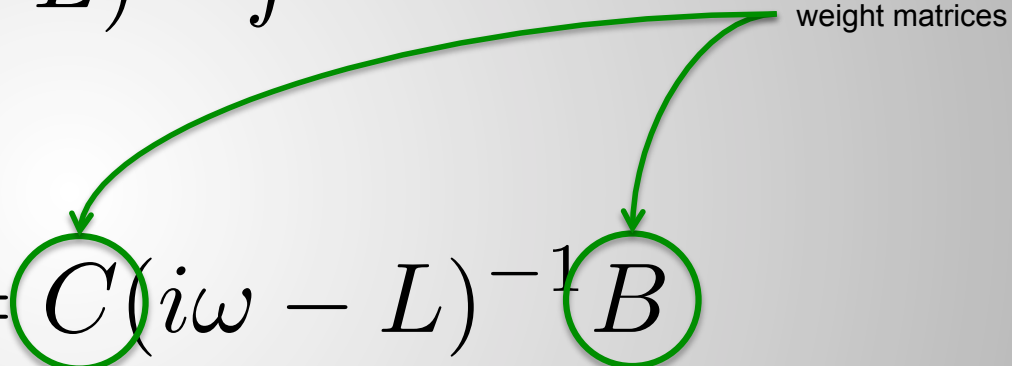
smoke visualization of boundary layer transition

It is often instructive to compute the energy amplification component-wise.

Recall the response to harmonic forcing

$$\hat{q}_p = (i\omega - L)^{-1} \hat{f}$$

and define a *transfer function*

$$\mathcal{H}(\alpha, \beta, \omega) = C(i\omega - L)^{-1} B$$


weight matrices

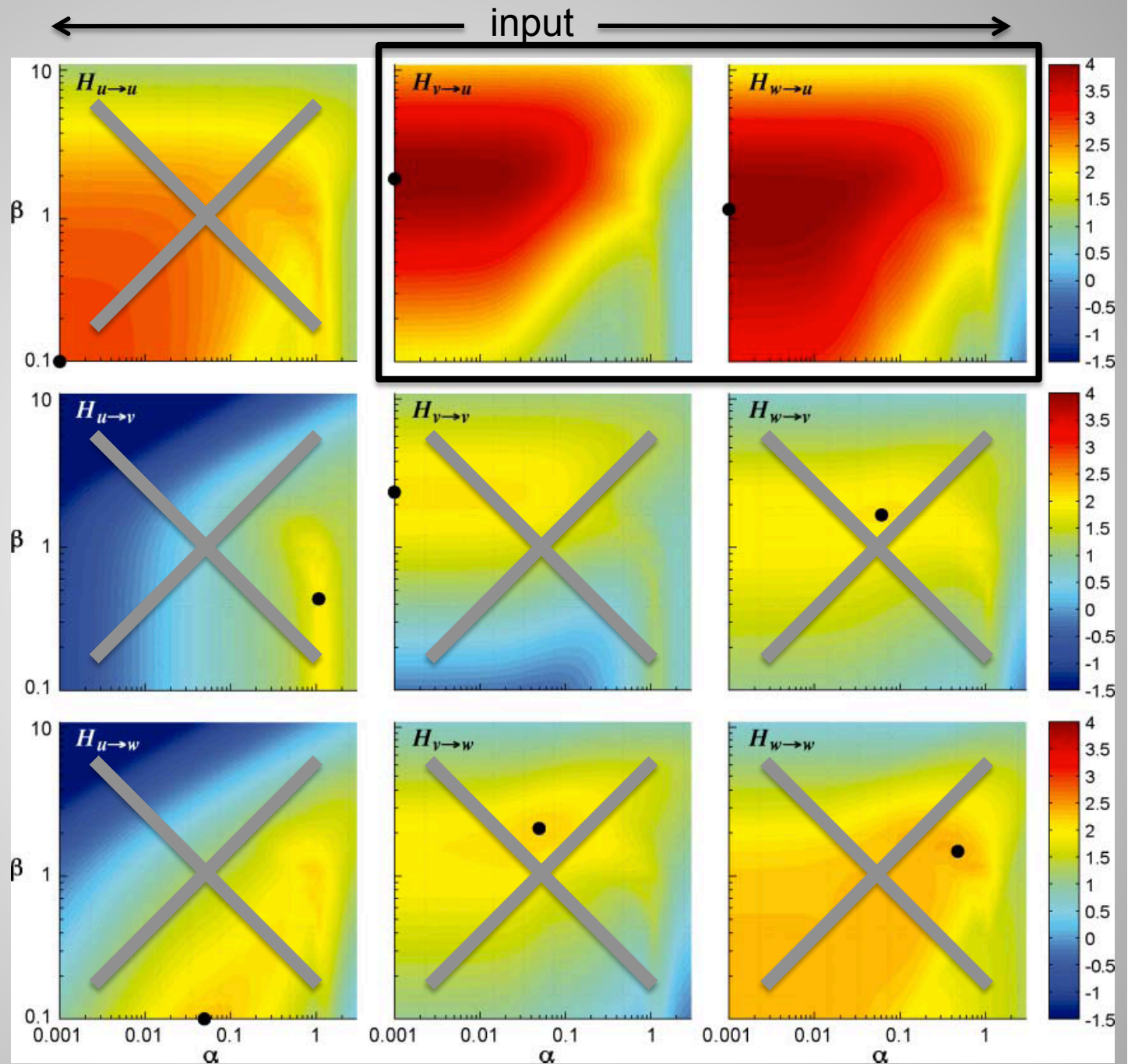
and take the worst-case amplification (over all frequencies)

$$\|\mathcal{H}\|_{\infty}(\alpha, \beta) = \max_{-\infty < \omega < \infty} \sigma_{\max}(\mathcal{H})$$

input-output analysis

$$\|\mathcal{H}\|_{\infty}(\alpha, \beta) = \max_{-\infty < \omega < \infty} \sigma_{\max}(\mathcal{H})$$

output



Generalizations

time-periodic flow



pseudo-Floquet analysis

In many industrial applications (e.g., turbomachinery) the mean flow is periodic in time due to an oscillatory pressure gradient

We have

$$\frac{d}{dt}q = L(t)q$$

$$L(t + T) = L(t)$$

period T

with the formal solution

$$\text{final solution } q(t) = A(t)q_0 \text{ initial condition}$$

propagator

Generalizations

time-periodic flow



pseudo-Floquet analysis

periodicity requires that

$$A(t + T) = A(t) \quad A(T) = A(t) C$$

monodromy matrix
(mapping over one period)

$$q_n = C q_{n-1} = C^n q_0$$

initial state

Generalizations

time-periodic flow



pseudo-Floquet analysis

$$q_n = C q_{n-1} = C^n q_0$$

energy amplification from period to period

$$G_n^2 = \max_{q_0} \frac{\|q_n\|^2}{\|q_0\|^2} = \max_{q_0} \frac{\|C^n q_0\|^2}{\|q_0\|^2} = \|C^n\|^2$$

The eigenvalues of C are known as Floquet multipliers.

Question: Do the Floquet multipliers describe the behavior of $\|C^n\|^2$?

Generalizations

time-periodic flow



pseudo-Floquet analysis

as before, let us compute bounds

$$\rho^{2n} \leq \|C^n\|^2 \leq \kappa^2(S) \rho^{2n}$$

largest Floquet
multiplier

Conclusion: only for normal monodromy matrices does the largest Floquet multiplier describe the behavior from period to period

for nonnormal monodromy matrices there is a potential for transient amplification from period to period; only the asymptotic behavior $n \rightarrow \infty$ is governed by the largest Floquet multiplier

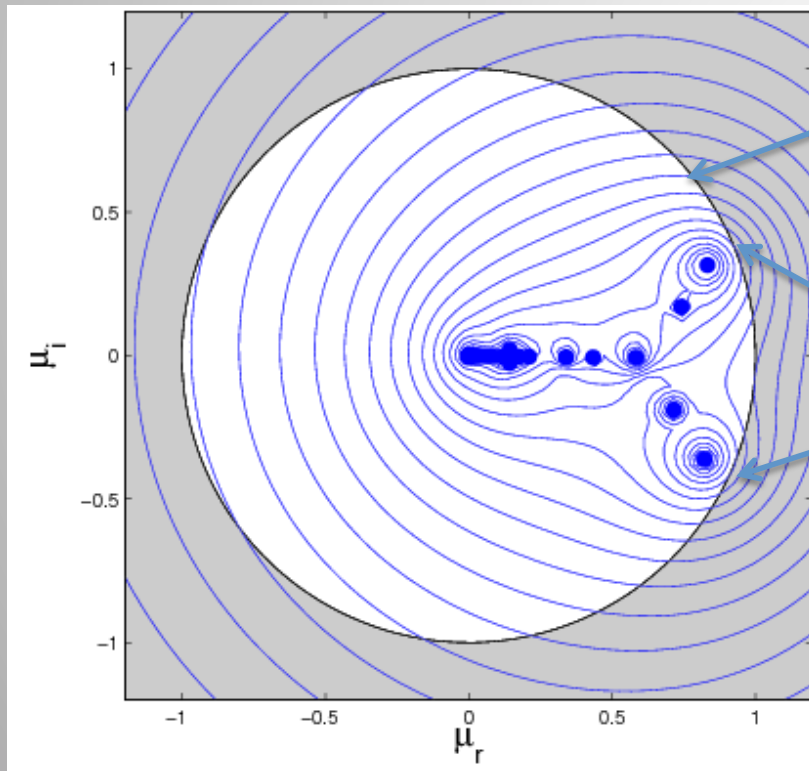
Generalizations

time-periodic flow



pseudo-Floquet analysis

Example: pulsatile channel flow



all Floquet multipliers are inside the unit disk indicating asymptotic stability (contractivity) as $n \rightarrow \infty$

the resolvent contours reach outside the unit disk suggesting initial transient growth from period to period

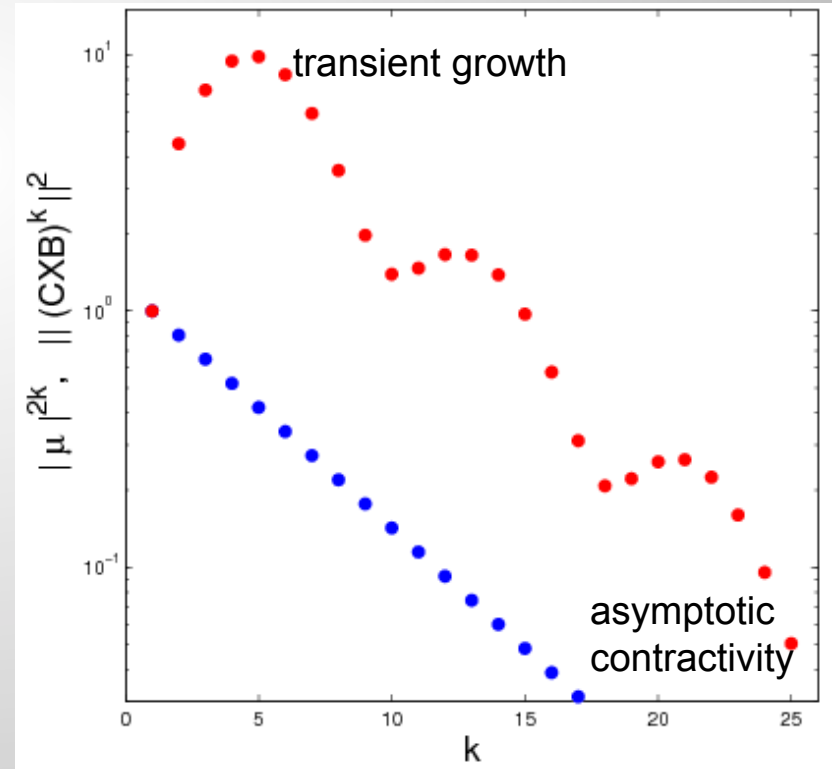
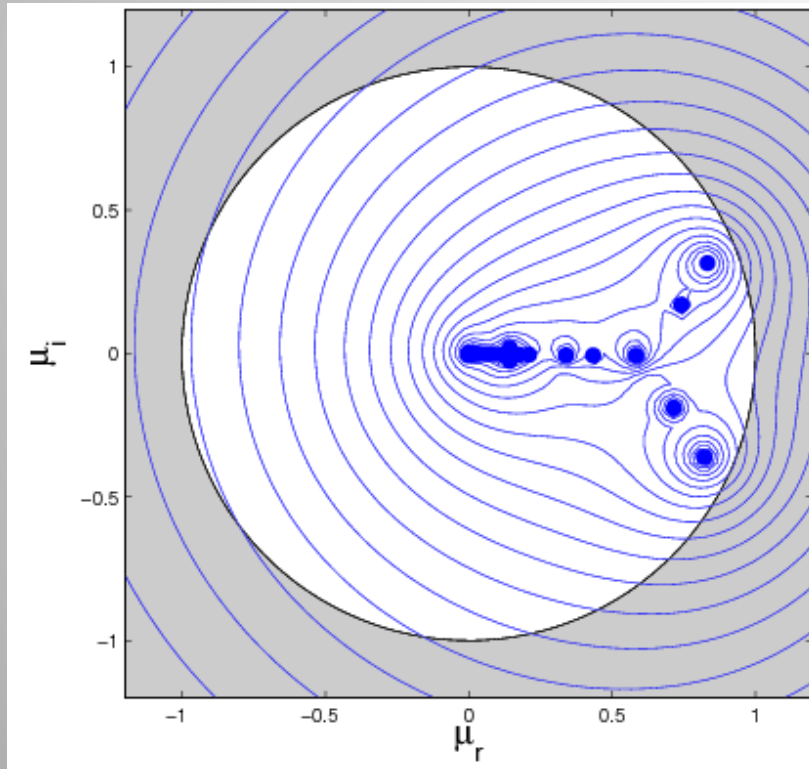
Generalizations

time-periodic flow



pseudo-Floquet analysis

Example: pulsatile channel flow



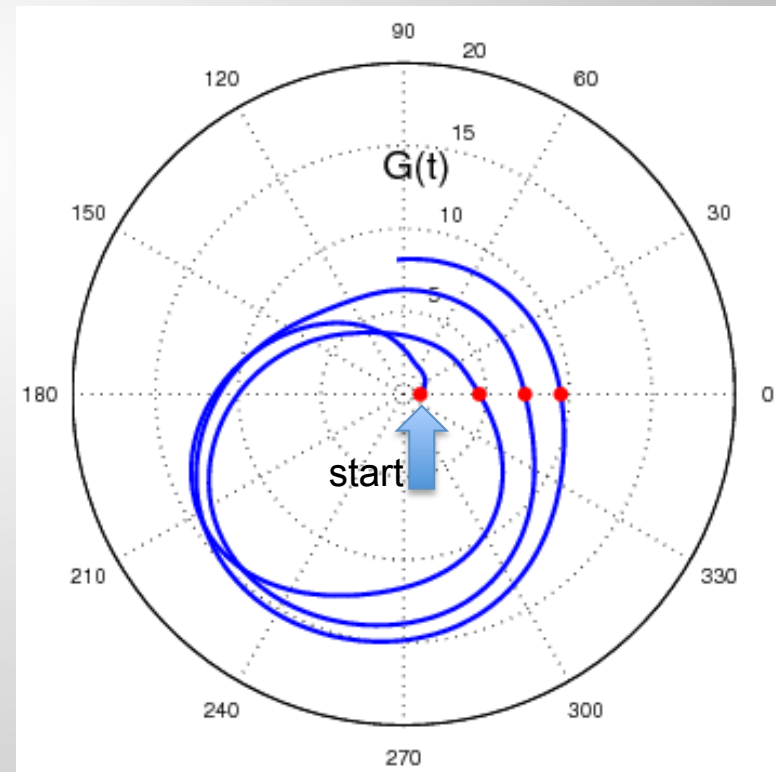
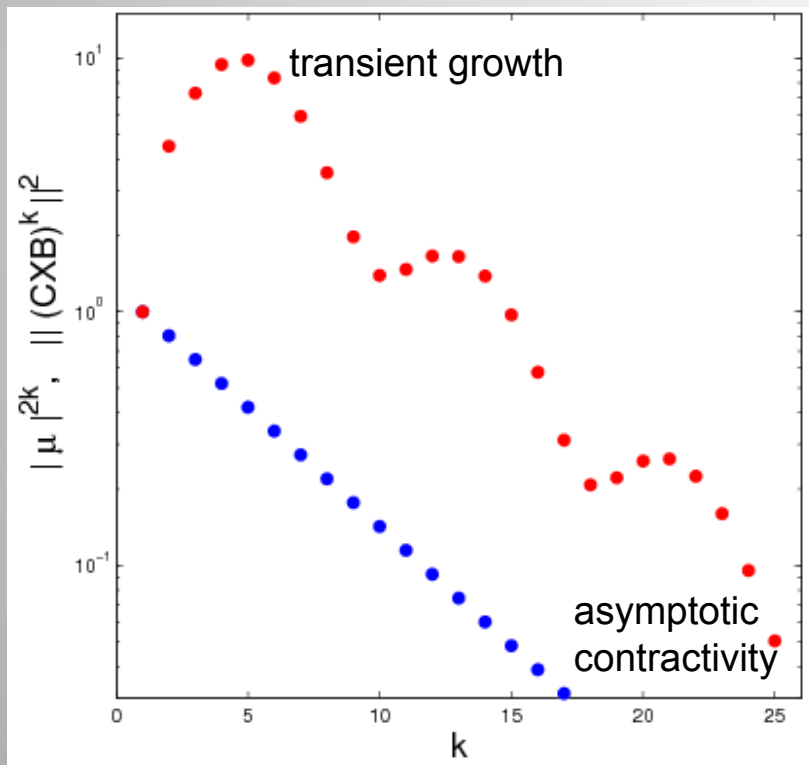
Generalizations

time-periodic flow



pseudo-Floquet analysis

Example: pulsatile channel flow



Summary

- Nonnormal operators are ubiquitous in fluid dynamics and related fields.
- In many cases multimodal effects are more relevant than single-mode phenomena.
- Nonnormal analysis is computationally more involved; extensions to non-generic cases (time-dependent, nonlinear, stochastic, multi-dimensional) are possible.
- Nonmodal analysis gives a more accurate picture of fluid flow behavior.